iScience

CellPress
OPEN ACCESS

Review

Phase Change Materials for Electro-Thermal Conversion and Storage: From Fundamental Understanding to Engineering Design

Xiao Chen,[1,*] Zhaodi Tang,[2] Hongyi Gao,[2] Siyuan Chen,[2] and Ge Wang[1,2,*]

Advanced functional electro-thermal conversion phase change materials (PCMs) can efficiently manage the energy conversion from electrical energy to thermal energy, thereby playing a significant role in sustainable energy utilization. Considering the inherent insulating properties of pristine PCMs, electrically conductive supporting materials are widely used to encapsulate PCMs to prepare composite PCMs for electro-thermal conversion and storage. Herein, we comprehensively review the recent advances in different electro-thermal conversion PCMs, mainly including carbon-based PCMs (carbon nanotubes [CNTs], graphene, biomass-derived carbon, graphite, highly graphitized carbon, and metal organic frameworks [MOFs]-derived carbon) and MXene-based PCMs. This review aims to provide an in-depth understanding of the electrothermal conversion mechanism and the relationships between structure design (random and array-oriented structure or single and hybrid supporting materials) and electrothermal properties, thereby contributing profound theoretical and experimental bases for the construction of high-performance electro-thermal conversion PCMs. Finally, we highlight the current challenges and future prospects.

INTRODUCTION

Multiple energy sources are available in nature. Energy conversion and storage is critical for actual energy utilization according to scenario requirements. For instance, batteries and supercapacitors can convert chemical energy into electrical energy and store it (Hosaka et al., 2020; Liu et al., 2020b). Solar cells can convert solar energy into electrical energy and store it (Back et al., 2020; Bertoluzzi et al., 2020). Photocatalysts can convert solar energy into chemical energy and store it (Cao et al., 2020; Gao et al., 2020). Electrocatalysts can convert electrical energy into chemical energy and store it (Göhl et al., 2020; Tian et al., 2020). Therefore, energy conversion and storage technologies and the development of new energy sources are equally important. Solar energy is considered as one of the most potential renewable and sustainable energy sources among the various energy sources because of its abundant, universal, and clean features. Therefore, photo-thermal conversion phase change materials (PCMs) that are capable of reversibly storing and releasing tremendous thermal energy during the isothermal phase transition (Chen et al., 2019a, 2019b, 2020; Lyu et al., 2019a, 2019b) are the most commonly investigated among the energy conversion PCMs (Allahbakhsh and Arjmand, 2019; Latibari and Sadrameli, 2018; Qiu et al., 2019; Zhang et al., 2019c; Zhou et al., 2015). Considering the intermittent deficiency of sunlight, emerging electro-thermal conversion PCMs are a better solution.

Recently, electro-thermal conversion and storage technology-based functional PCMs have shown a great potential in the thermal management of power vehicles, electronic devices, and off-peak electricity storage systems (Aftab et al., 2019; Chen et al., 2012; Li et al., 2018, 2020b; Lu et al., 2019; Maleki et al., 2019; Umair et al., 2019b; Wang et al., 2017b; Xue et al., 2019, 2020). The electrical conductivity and thermal conductivity of PCMs are two important factors affecting their electro-thermal conversion capacity. However, the inherent low electrical conductivity (10^{7}–10^{12} Ω·m) and thermal conductivity (0.1–0.4 W/mK) of pristine PCMs severely restrict their electro-thermal energy conversion utilization (Cheng et al., 2020; Liu et al., 2020a; Sun et al., 2020; Zhang et al., 2019c). One prospective solution is that highly conductive supporting materials are introduced into PCMs to prepare composite PCMs. Currently, the development of high-performance electrothermal composite PCMs has become a research focus. Many studies have proven that the introduction of carbonaceous materials (such as carbon nanotubes [CNTs] [Aftab et al., 2019],

[1]Institute of Advanced Materials, Beijing Normal University, Beijing 100875, PR China

[2]Beijing Advanced Innovation Center for Materials Genome Engineering, Beijing Key Laboratory of Function Materials for Molecule & Structure Construction, School of Materials Science and Engineering, University of Science and Technology Beijing, Beijing 100083, PR China

*Correspondence: xiaochen@bnu.edu.cn (X.C.), gewang@mater.ustb.edu.cn (G.W.)

https://doi.org/10.1016/j.isci.2020.101208

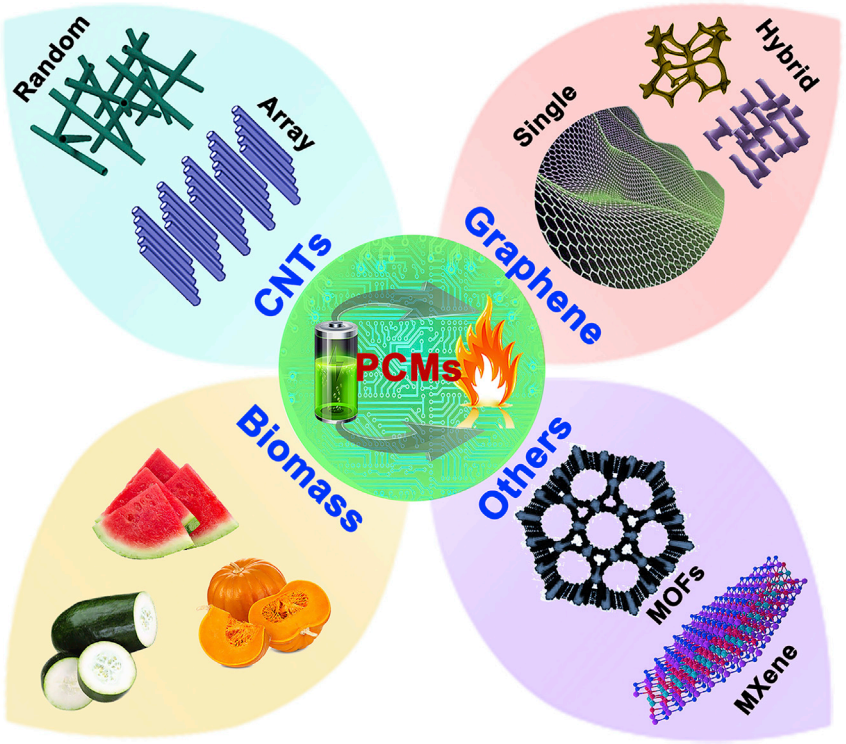

Figure 1. Overview of Main Supporting Materials of Composite PCMs for Electro-Thermal Conversion and Storage

graphene [Li et al., 2018], biomass-derived carbon [Umair et al., 2019b], graphite [Chen et al., 2015], expanded graphite [Tabassum et al., 2015], and highly graphitized carbon [Maleki et al., 2019]) into PCMs can effectively realize the electro-thermal conversion of PCMs owing to their high electrical and thermal conductivities. Generally, a small amount of carbon materials can form a conductive percolation network to enhance the conductivity of PCMs. In addition to the aforementioned conductive additives, some advanced conductive materials have recently emerged in the field of electro-thermal conversion PCMs, such as boron nitride (BN) (Yang et al., 2020), MXene (Lu et al., 2019), and MOFs-derived carbon (Li et al., 2020a). However, electrothermal composite PCMs-based BN, MXene, and MOFs-derived carbon are very rare, which need more exploration and research in the future.

To the best of our knowledge, the current reviews mainly summarize thermal conductivity enhancement of PCMs (Ibrahim et al., 2017; Lin et al., 2018; Qureshi et al., 2018; Wu et al., 2019b; Yuan et al., 2020), thermal properties of PCMs (Arivazhagan et al., 2020; Leong et al., 2019; Li and Mu, 2019; Tong et al., 2019), thermal storage applications of PCMs (Huang et al., 2019; Nazir et al., 2019; Shchukina et al., 2018; Umair et al., 2019a), nanoporous shape-stabilized PCMs (Aftab et al., 2018; Feng et al., 2019; Gao et al., 2018), microencapsulated PCMs (Drissi et al., 2019; Konuklu et al., 2015; Liu et al., 2016), photo-thermal conversion PCMs (Latibari and Sadrameli, 2018; Qiu et al., 2019; Zhang et al., 2019c), etc. However, a comprehensive review of electrothermal composite PCMs for energy conversion and storage has not been presented. Herein, we provide a comprehensive perspective of the recent advances in electro-thermal conversion PCMs from the fundamental understanding to engineering design (Figure 1). This review aims to deeply understand the electro-thermal conversion mechanism and the relationships between structure design and electrothermal properties, thereby providing insightful theoretical and experimental bases for the construction of high-performance electro-thermal conversion PCMs. Finally, the perspectives and current challenges are also highlighted.

MECHANISM OF ELECTRO-THERMAL CONVERSION AND STORAGE OF PCMS

In general, pristine PCMs typically have intrinsic low thermal conductivity (0.1–0.4 W/mK) and high electrical resistivity (10^7–10^{12} $\Omega \cdot m$) (Sun et al., 2020; Zhang et al., 2019c). Hence, pristine PCMs are insulating in

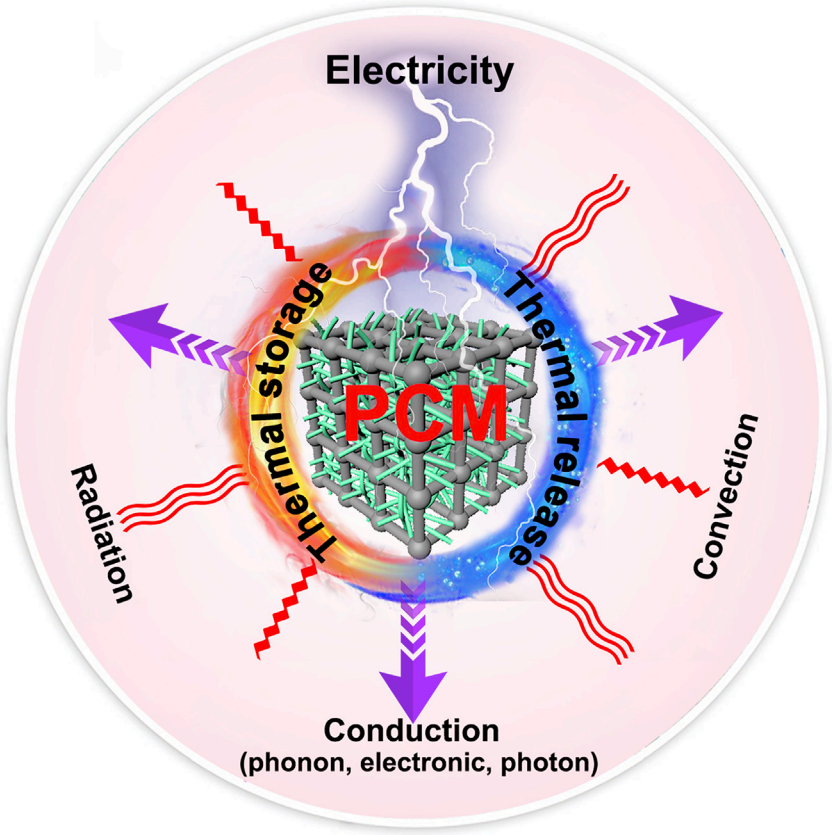

Figure 2. Mechanism of Electro-Thermal Conversion and Storage of PCMs

nature, and their electro-thermal conversion and storage process is unlikely to be triggered directly. The most feasible solution is to encapsulate PCMs using highly electrically and thermally conductive supporting materials. The resultant electro-thermal composite PCMs mainly involve the following main stages: electro-thermal conversion, heat transfer, and melting/crystallization. The corresponding mechanism is shown in Figure 2.

The basic electric-thermal conversion mechanism is as follows. When electric current flows through conductive PCMs, the generated Joule heat is released. Joule heat is generated when moving electrons collide with other molecules or groups (Zhang et al., 2019c). Then, the released Joule heat is absorbed by PCMs and is eventually stored in the form of latent heat. Heat transfer phenomenon is very common in nature. Its three fundamental modes are thermal conduction, thermal convection, and thermal radiation. Thermal conduction usually emerges inside solid matter or at the contact surface of solid-solid/liquid matter. Thermal convection generally emerges inside liquid or gas matter. All matter with a temperature exceeding absolute zero can emit thermal radiation. Comparatively, thermal conduction mode is the most effective and common, which is also the dominant heat transfer mode in PCMs. The majority of PCMs are solid materials before their phase change. In general, their thermal conduction mechanisms of solid PCMs are further divided into three categories: phonon heat conduction, electronic heat conduction, and photon heat conduction, corresponding to lattice vibration waves, free electrons, and electromagnetic radiation, respectively (Meschke et al., 2006; Yuan et al., 2020). Comparatively, photons only account for a relatively weak part for most matter. Therefore, electronic heat conduction and photon heat conduction are main mechanisms (Yu et al., 2010). For metallic materials, electronic heat conduction is dominant through the interaction between free electrons. For nonmetallic materials, photon heat conduction is dominant through the interaction between lattice vibration waves. It should be noted that it is difficult to explain the thermal conduction mechanism of all PCMs with one theory.

The reversible thermal storage (melting) and release (crystallization) of PCMs are realized through the order-disorder structure transformation of PCMs molecular arrangement. In the endothermic process, the temperature of composite PCMs is increased sharply when a voltage is input in the initial stage. The converted heat from electrical energy is stored in the form of sensible heat. During this process, PCMs maintain a solid state. In the second stage, the slope of temperature-time plots gradually drops until an inflection point. In this case, PCMs start to undergo a solid-liquid phase change and the converted heat from electrical energy is stored in the form of latent heat. As observed from the temperature-time plots, there is a tilted temperature plateau at this stage, corresponding to the melting process of PCMs. After phase transition terminates, the temperature of composite PCMs is increased sharply again until the equilibrium state. This stage is the same as the first stage, and the converted heat from electrical energy is stored in the form of sensible heat again. In the exothermic process, the temperature immediately drops to the freezing temperature of PCMs after terminating the applied voltage. At this time, another tilted temperature plateau is observed again, corresponding to the crystallization process of PCMs.

The electro-thermal conversion and storage efficiency (η) can be calculated through $\eta = m\Delta H/UIt$, in which m is the total mass, ΔH is the phase change enthalpy, U and I are the applied voltage and current, and t is the complete phase transition time. The starting and finishing points of the phase transition can be determined using a tangent method from the temperature-time plots. Here, it is worth mentioning that not any voltage can initiate the electro-thermal conversion but only appropriate voltage can initiate the electro-thermal conversion for different composite PCMs. Below the critical voltage, the electro-thermal conversion process of composite PCMs cannot be initiated, corresponding no tilted temperature plateau. In contrast, a higher applied voltage would result in a higher electro-thermal conversion efficiency. This is because the complete phase change period is shorted and the corresponding convection heat loss from the exposed composite PCMs to the environment is reduced, thus resulting in an improved efficiency. Therefore, the electro-thermal conversion efficiency could be further enhanced using a suitable heat-sealing technology to reduce even prevent the heat dissipation to the environment.

ELECTRO-DRIVEN COMPOSITE PCMS FOR ENERGY CONVERSION AND STORAGE

It is universally acknowledged that pristine PCMs are insulators with poor electrical conductivity and thermal conductivity (Chen et al., 2018, 2020; Zhang et al., 2019c). Therefore, pristine PCMs are impossible to directly convert electrical energy into thermal energy. Generally, highly conductive fillers or structures can be introduced into PCMs to achieve electro-thermal conversion and storage. The conventional conductive fillers used for electro-thermal conversion are metals and metal alloys. Comparatively, highly conductive carbonaceous materials (such as CNTs, graphene, biomass-derived carbon, MOFs-derived carbon, graphite, expanded graphite, and highly graphitized carbon) are found to be efficient alternatives, which are the focus of this review (Table 1). In this section, we comprehensively review the influence of random and array-oriented structure, or single and hybrid supporting materials on the electro-thermal conversion and storage properties of composite PCMs. It is worth mentioning that the working voltage and electro-thermal conversion efficiency are two key factors of electro-thermal conversion PCMs. Reducing the working voltage while maintaining high electro-thermal conversion efficiency to improve their application security will become the focus of future attention.

CNTs-Based Composite PCMs for Electro-Thermal Conversion and Storage

Theoretically, single/multi-wall CNTs have an extremely high electrical conductivity and thermal conductivity (Avery et al., 2016; Gulotty et al., 2013; Huxtable et al., 2003). These prominent conductive features of CNTs make them promising supporting materials candidates for electro-thermal conversion PCMs. Herein, random and array-oriented CNTs-based composite PCMs are discussed and analyzed in electro-thermal conversion and storage.

Random CNTs-Based Composite PCMs

Alkyl acrylates are a type of organic PCMs with high phase change enthalpy, adjustable phase change temperature by changing the number of carbon atoms, and low or almost no supercooling degree (Cao et al., 2017). Cao et al. (2019a) fabricated hexadecyl acrylate-functionalized random single/multi-wall CNTs (HDA-g-SWCNTs, HDA-g-MWCNTs)-based composite PCMs via a solvent-free Diels-Alder (DA) reaction. During the DA reaction, [4 + 2] cycloaddition products are formed by the reaction between the conjugated double bonds of SWCNTs/MWCNTs and unsaturated double bonds of HDA (Fei et al., 2018). Meanwhile,

Supporting Materials	Types of PCMs	Loading (wt%)	Melting Point (°C)	Melting Enthalpy (J/g)	Electrical Conductivity (S/m)	Thermal Conductivity (W/mK)	Input Voltage (V)	Conversion Efficiency (%)	Reference
CNTs	Hexadecyl acrylate	–	36.7	52.0	718.0	0.47	–	–	Cao et al., 2019a
CNTs	Hexadecyl acrylate	–	38.0	40.0	389.0	0.88	–	–	Cao et al., 2019a
CNTs	Paraffin	80	–	–	–	1.20	1.5	40.6	Chen et al., 2012
CNTs	Paraffin	80	–	–	–	1.20	1.75	52.5	Chen et al., 2012
CNTs	PEG2000	80	33.2	89.8	–	0.91	1.5	58.3	Sun et al., 2020
CNTs	PEG2000	80	33.2	89.8	–	0.91	2.0	70.2	Sun et al., 2020
CNTs	n-Eicosane	90	34.5	217.0	–	–	1.7	38.9	Liu et al., 2013
CNTs	n-Eicosane	90	43.0	217.3	–	–	1.3	74.7	Liu et al., 2013
CNTs	Polyurethane	90	59.4	132.0	–	2.40	1.5	49.0	Aftab et al., 2019
CNTs	Polyurethane	90	59.4	132.0	–	2.40	2.0	94.0	Aftab et al., 2019
Graphene	Hexadecyl acrylate	42	32.7	57.0	219.0	3.96	–	–	Cao et al., 2019b
Graphene aerogel	Paraffin	94	47.8	193.7	258.7	2.99	1.5	50.5	Li et al., 2016
Graphene aerogel	Paraffin	94	47.8	193.7	258.7	2.99	3.0	85.4	Li et al., 2016
Graphene/rGO	Paraffin	95.5	43.8	155.5	278.7	1.46	2.9	62.5	Xue et al., 2019
Graphene aerogel	PEG4000	98.8	57.4	92.1	–	–	10.0	67.2	Zhou et al., 2019
Graphene aerogel/ halloysite nanotubes	PEG4000	98.8	57.4	103.3	–	–	10.0	66.3	Zhou et al., 2019
rGO/BN	PEG10000	84.8	59.5	164.1	–	1.06	7.0	87.9	Yang et al., 2020
Graphene/cellulose	PEG6000	–	–	182.6	–	1.03	–	–	Wei et al., 2019
Graphene/cellulose	PEG6000	95	61.7	178.9	6.2	0.26	20.0	66.1	Wu et al., 2019a
Graphene/cellulose	Paraffin	–	46.7	147.9	–	1.42	–	–	Xue et al., 2020
GO/CNTs	PEG1000	85	33.9	120.7	–	0.37	7.0	63.0	Guo et al., 2018
GO/CNTs	PEG1000	85	33.9	120.7	–	0.37	6.6	70.0	Guo et al., 2018
Carbon cloth	Paraffin/ polyurethane	49	–	93.6	374.0	–	3.0	34.9	Umair et al., 2019b
Carbon cloth		49	–	93.6	374.0	–	4.0	67.4	Umair et al., 2019b

Table 1. Summary of Electro-Thermal Conversion PCMs

(Continued on next page)

Supporting Materials	Types of PCMs	Loading (wt%)	Melting Point (°C)	Melting Enthalpy (J/g)	Electrical Conductivity (S/m)	Thermal Conductivity (W/mK)	Input Voltage (V)	Conversion Efficiency (%)	Reference
	Paraffin/ polyurethane								
Carbon aerogels	Paraffin	95	53.5	115.2	3.4	–	15.0	71.4	Li et al., 2014
Hollow carbon fiber	Paraffin	85	39.2	182.2	19.6	0.42	3.0	81.1	Umair et al., 2020
MXene	PEG4000	77.5	–	131.2	10.4	2.05	–	–	Lu et al., 2019
Acetylene black	PEG2000	80	55.7	78.5	3.3	1.42	1.5	29.7	Zhang et al., 2018
Acetylene black	PEG2000	80	55.7	78.5	3.3	1.42	2.5	64.7	Zhang et al., 2018
Expanded graphite	Methyl stearate	80	33.4	147.0	–	3.60	1.4	47.0	Tabassum et al., 2015
Expanded graphite	Methyl stearate	80	33.4	147.0	–	3.60	1.7	72.0	Tabassum et al., 2015
Graphite foam	PEG4000/ polyurethane	76	41.0	64.5	–	3.50	1.4	69.0	Chen et al., 2015
Graphite foam	PEG6000/ polyurethane	82	42.5	76.1	–	3.40	1.4	88.0	Chen et al., 2015
Graphite foam	PEG8000/ polyurethane	81	46.1	80.3	1.0	3.40	1.4	48.0	Chen et al., 2015
Graphite foam	Polyurethane	73	43.8	60.3	–	10.86	1.7	79.0	Wu et al., 2017
Graphite foam	Polyurethane	73	43.8	60.3	–	10.86	1.8	85.0	Wu et al., 2017
Graphitic carbon foam	PEG6000	91	62.8	163.9	–	–	3.0	52.0	Maleki et al., 2019
Graphitic carbon foam	PEG6000	91	62.8	163.9	–	–	3.6	85.0	Maleki et al., 2019
Graphitic carbon foam	Paraffin	87	57.1	120.2	–	–	3.0	56.0	Maleki et al., 2019
Graphitic carbon foam	Paraffin	87	57.1	120.2	–	–	3.6	74.0	Maleki et al., 2019

Table 1. Continued

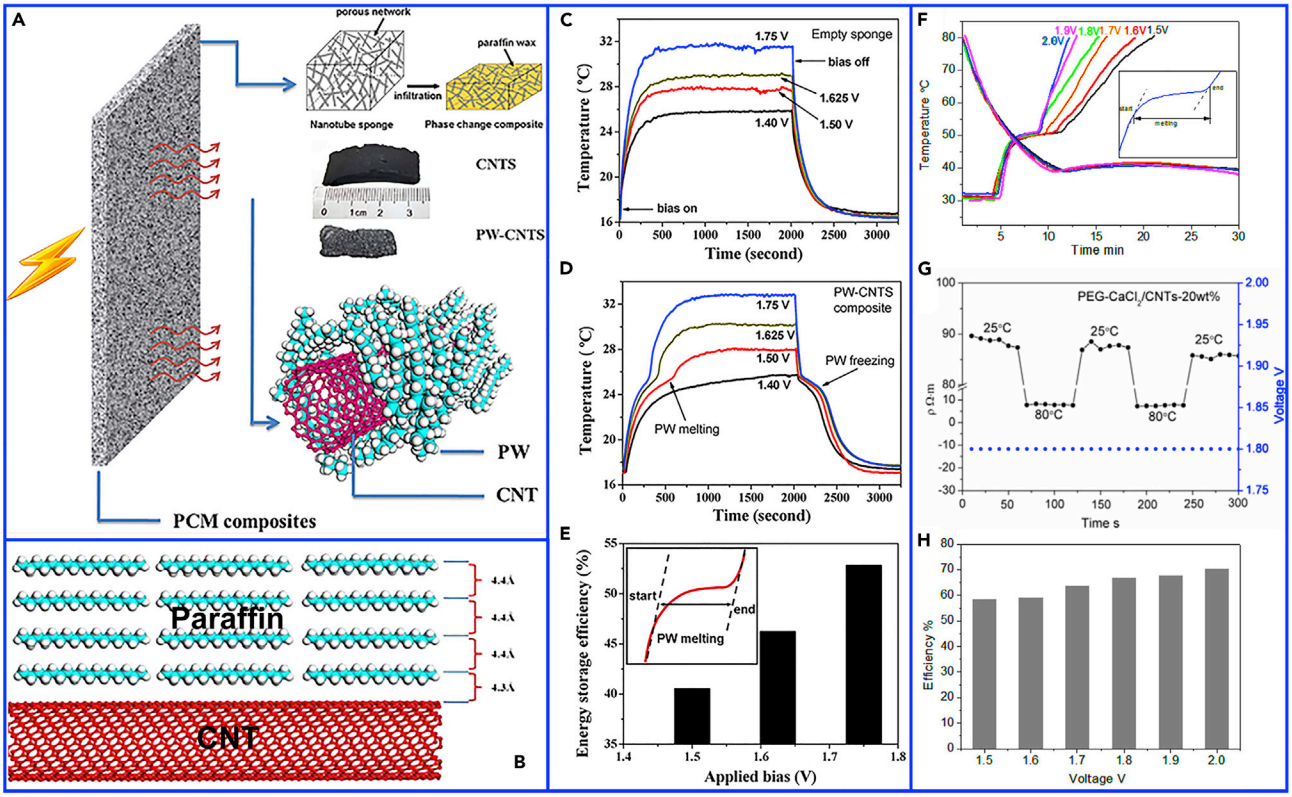

Figure 3. Random CNTs-Based Composite PCMs

(A) Schematic diagram of the electro-thermal conversion of CNTs-based composite PCMs.

(B) Contact illustration between CNTs and paraffin molecules.

(C and D) Temperature evolution curves of an empty sponge and composite PCMs under different voltages.

(E) Electro-thermal conversion efficiencies of composite PCMs under different voltages. Adapted with permission from Chen et al. (2012). Copyright 2012, American Chemical Society.

(F) Temperature evolution curves of composite PCMs under different voltages.

(G) Resistivity curve of composite PCMs in the crystalline/liquid state.

(H) Electro-thermal conversion efficiencies of composite PCMs under different voltages. Adapted with permission from Sun et al. (2020). Copyright 2020, Elsevier.

the sp^2 hybridized carbon of SWCNTs/MWCNTs is transformed to sp^3 hybridized carbon and HDA molecules are covalently grafted onto the surface of SWCNTs/MWCNTs (Yuan et al., 2012). Generally, the electrical conductivity of individual SWCNTs/MWCNTs may even drop significantly several times when they are covalently functionalized with sp^3 rehybridization. However, the electrical conductivities of these covalently grafted HDA-g-SWCNTs (718 S/m) and HDA-g-MWCNTs (389 S/m) are significantly improved. Moreover, the thermal conductivities of HDA-g-SWCNTs (0.47 W/mK) and HDA-g-MWCNTs (0.88 W/mK) are 134% and 339% higher than that of pristine HDA (0.20 W/mK). Therefore, HDA-g-SWCNTs/HDA-g-MWCNTs composite PCMs have a certain electro-thermal energy conversion and storage performance. This function can effectively apply PCMs to the thermal buffer in integrated circuits.

However, the actual fabrications of CNTs-based composite PCMs are usually hindered by several factors. For example, random CNTs tend to aggregate when the weight percentage of CNTs is higher in the composite PCMs. The overall structure of composite PCMs is even electrically insulated when the loading content of PCMs is relatively high; therefore, these composite PCMs are impossible to realize electro-thermal conversion and storage. To overcome these deficiencies of CNTs-based composite PCMs, Chen et al. (2012) prepared deformable CNTs sponge to encapsulate paraffin for electro-thermal conversion (Figure 3A). Interestingly, the prepared CNTs sponge can be compressed to arbitrary shapes with large strains and then the original shape can be recovered without obvious deformation. The close contact between paraffin and CNTs due to the excellent affinity and uniform interpenetration effect is essential to enhance

the thermal and electrical conductivity of composite PCMs (Figure 3B). Consequently, the composite PCMs with 80 wt% paraffin exhibit a high thermal conductivity of 1.2 W/mK with a 6-fold increase compared with pristine paraffin. It is also worth mentioning that the composite PCMs with 91 wt% paraffin have a phase change enthalpy of 138.2 J/g, which is higher than pristine paraffin. The increased thermal conductivity and phase change enthalpy are attributed to the remarkable intermolecular C-H$\cdots\pi$ interactions between CNTs and paraffin based on the Lennard-Jones potential (Kim et al., 2000; Shaikh et al., 2008; Tarakeshwar et al., 2001; Tsuzuki et al., 2000). The other researches have also confirmed that the introduced CNTs can evidently increase the phase change enthalpy of PCMs (Wang et al., 2017a; Zhu et al., 2019). More importantly, a critical voltage (1.5 V) can directly trigger the electro-thermal energy conversion and storage (40.6%) of CNTs-based composite PCMs owing to the highly conductive CNTs network (Figures 3C–3E). At a higher voltage (1.75 V), the electro-thermal conversion efficiency is increased to 52.5% because higher voltage can short the phase change period and reduce the convection heat loss between composite PCMs and the environment.

In addition to single organic PCMs-based composite PCMs for electro-thermal conversion, Sun et al. (2020) prepared organic-inorganic hybrid electrothermal composite PCMs (PEG-$CaCl_2$/CNTs, polyethyleneglycol) (Figure 3F) using the coordination chemistry and ligand substitution techniques. In the PEG-$CaCl_2$/CNTs composite PCMs, the formed coordinate covalent bonds can effectively improve the mechanical strength. The thermal conductivity and electrical resistivity of PEG-$CaCl_2$/CNTs composite PCMs with 20 wt% CNTs are increased by 252% and reduced from 9,500 to 90 U•m (Figure 3G), respectively. As a result, the electro-thermal conversion in the PEG-$CaCl_2$/CNTs-20 wt% composite PCMs could be triggered under a relatively low voltage of 1.5–2.0 V. The corresponding electro-thermal conversion efficiencies are 58.3% (1.5 V) and 70.2% (2.0 V), respectively, as shown in Figure 3H. Additionally, the phase change enthalpy is changed within 3.0% and electro-thermal conversion efficiency is changed within 5.0% after multiple thermal cycling tests, indicating the excellent thermostability.

Array-Oriented CNTs-Based Composite PCMs

Direct infiltration of PCMs into porous CNTs sponge or aerogel composed of randomly overlapped CNTs demonstrates a possibility to obtain electro-thermal conversion composite PCMs owing to the conductive CNTs network. However, the most difficult is that the distribution or distance of the random CNTs in the composite PCMs cannot be tailored. Compared with random CNTs sponge or aerogel, the array-oriented CNTs exhibit an ordered anisotropic structure and an enhanced electrically and thermally conductive network, thus showing greater potential in electro-thermal conversion.

Based on array-oriented construction concept, Liu et al. (2013) designed array-oriented CNTs/n-eicosane (C20) composite PCMs with modulated performances using a chemical vapor deposition technique (Figure 4A). The gap between the parallel CNTs can be filled by PCMs while keeping CNTs alignment and interconnection among the composite PCMs (Figure 4B). Therefore, array-oriented CNTs can accommodate the volume change during phase change without disturbing the alignment, whereas the empty array-oriented CNTs without incomplete filling using PCMs would cause volume shrinkage during the cooling. To tailor the areal density of CNTs, array-oriented CNTs are compressed perpendicular to aligned CNTs before C20 infiltration. Correspondingly, the areal density of CNTs is adjustable in the range from 3.75×10^6 to 6.45×10^6 per mm^2. Consequently, the compressed CNTs gaps can confine and align C20 molecules to form a preferential orientation along the gap. More importantly, the resistance is only about 10 Ω after C20 infiltration under a constant bias of 1 V. This high conductivity is conducive to triggering electro-thermal conversion of composite PCMs at a low voltage, which is difficult to realize in the conventional random CNTs-based composite PCMs. Compared with uncompressed composite PCMs, the compressed composite PCMs need a smaller driving voltage for electro-thermal conversion (Figures 4C–4F) owing to the reduced bulk resistance and enhanced heat transfer of dense CNTs array. The corresponding electro-thermal conversion efficiency of CNTs-C20-c40% composite is 74.7% at 1.3 V (Figure 4G). In addition, this array-oriented CNTs-based composite PCMs have superior thermal recycling stability (Figure 4H), which is attributed to the robust retention of array-oriented CNTs framework during the solid-liquid cycles.

To further improve the electro-thermal conversion efficiency of array-oriented CNTs-based composite PCMs, Aftab et al. (2019) employed array-oriented CNTs sponge (CNTS) to confine polyurethane (PU)-based PEG for electro-thermal conversion. The PU was first prepared by the reaction of hexamethylene diisocyanate and PEG under the catalyst, then impregnated into CNTS by solvent-assisted infiltration and vacuum drying

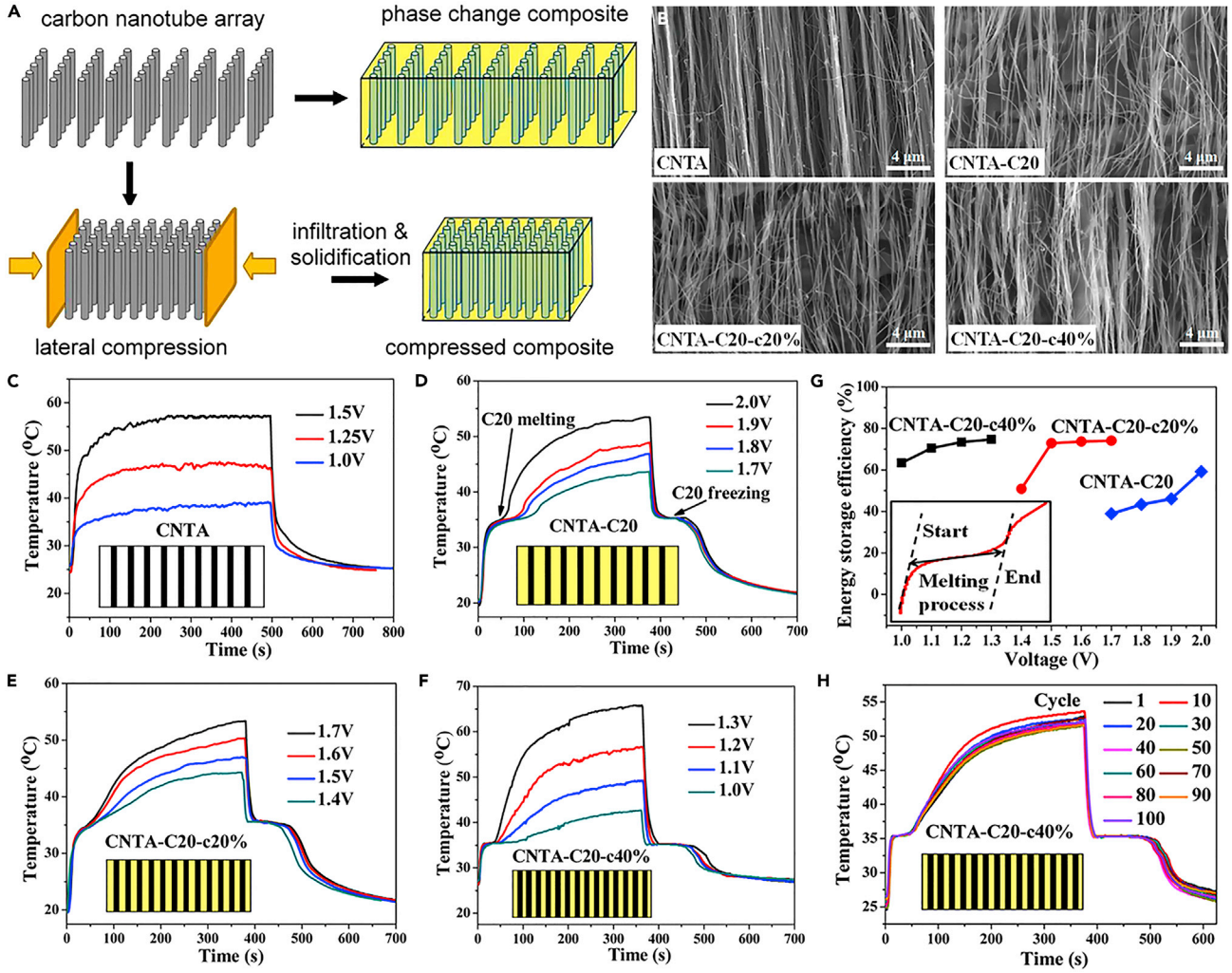

Figure 4. Array-Oriented CNTs-Based Composite PCMs

(A) Schematic diagram of compressible aligned CNT arrays and composite PCMs.

(B) SEM images of CNTs and CNTs/n-eicosane.

(C–F) Temperature evolution curves of CNTs and CNTs/n-eicosane.

(G) Electro-thermal conversion efficiencies of composite PCMs under different voltages.

(H) Cyclic stability of the electro-thermal conversion. Adapted with permission from Liu et al. (2013). Copyright 2013, American Chemical Society.

processes (Figure 5A). The resultant PU@CNTS composite PCMs have anisotropic and robust thermo-mechanical features (Figure 5B). PU@CNTS composite PCMs reveal an obvious volume shrinkage about 70%–80% compared with the original volume. This volume shrinkage ability benefits from the densification effect induced by the wetting and subsequent evaporation of solvent, which can accommodate PCMs volume expansion during the phase transition. More interestingly, the significant alignment of CNTs in the composite is still highly maintained owing to the opposite polarity of solidified PU, which can provide excellent thermal and electrical conduction channels. Consequently, PU@CNTS composite PCMs integrate a high phase change enthalpy (132 J/g), a high axial thermal conductivity of 2.40 W/mK (about 10 times higher than pristine PU), and a radial thermal conductivity of 0.95 W/mK. Therefore, PU@CNTS composite PCMs realize an ultra-high electro-thermal conversion efficiency of 94% at 2.0 V (Figures 5C–5E).

In general, array-oriented CNTs-based composite PCMs exhibit a higher electro-thermal conversion efficiency compared with random CNTs-based composite PCMs because array-oriented CNTs structure can provide a more efficient electrically and thermally conductive network. The current highest record of electro-thermal conversion efficiency is 94% at 2.0 V (Aftab et al., 2019).

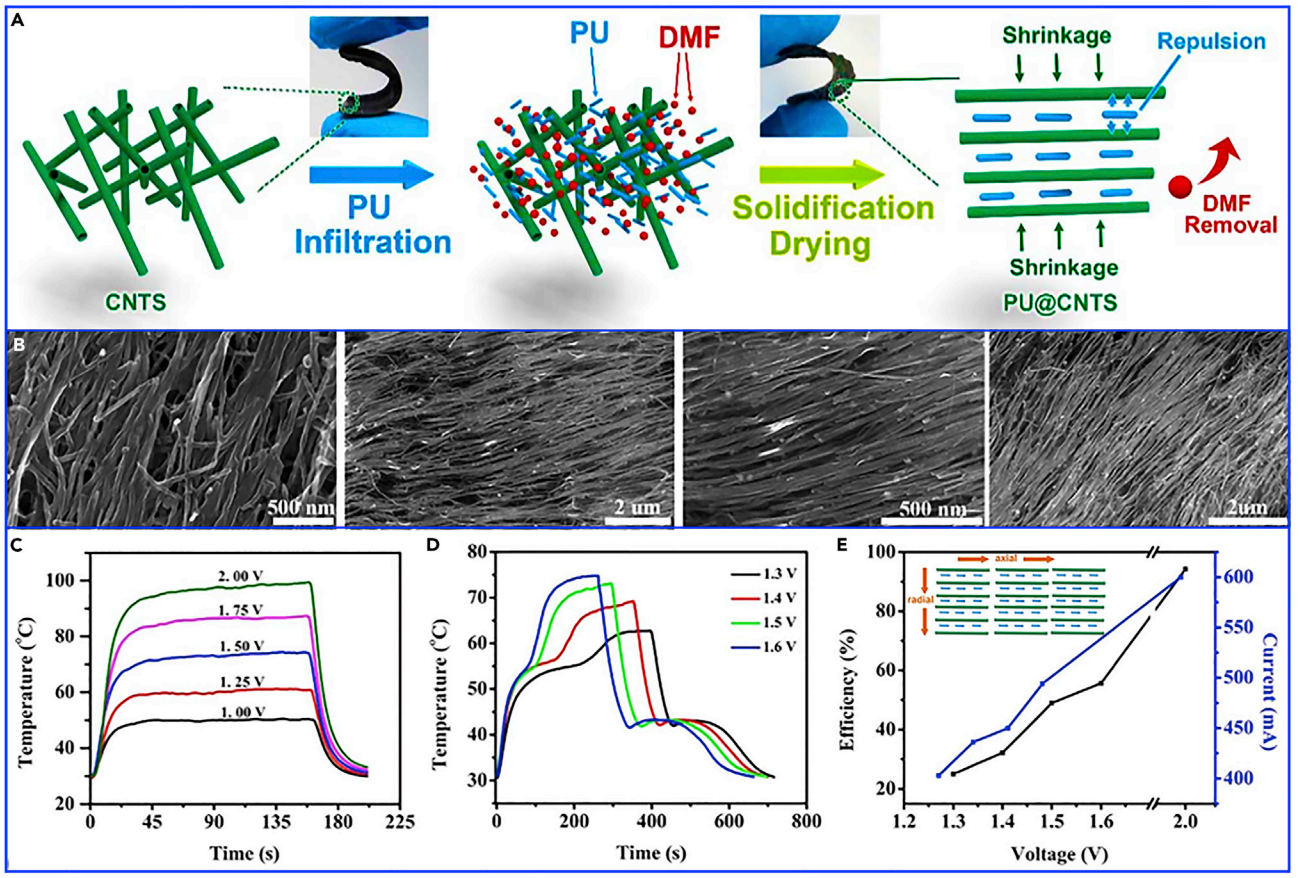

Figure 5. Array-Oriented CNTs-Based Composite PCMs

(A) Preparation diagram of composite PCMs.

(B) SEM images of composite PCMs from different perspectives.

(C) Temperature evolution curves of an empty CNTS under different voltages.

(D)Temperature evolution curves of composite PCMs under different voltages.

(E) Electro-thermal conversion efficiencies of composite PCMs under different voltages. Adapted with permission from Aftab et al. (2019). Copyright 2019, Elsevier.

Graphene-Based Composite PCMs for Electro-Thermal Conversion and Storage

Similar to CNTs, graphene with a sp^2-bonded single-layer 2D carbon sheet has an extremely high theoretical electrical conductivity and thermal conductivity (Balandin, 2011; Kim et al., 2016; Kong et al., 2019). These prominent conductive features make graphene and graphene derivatives promising supporting materials candidates of PCMs. The reliable production of graphene and graphene derivatives offers infinite possibilities for the manufacture of graphene-based electrothermal functional PCMs. Herein, single and hybrid graphene-based composite PCMs are discussed and analyzed in electro-thermal conversion and storage.

Single Graphene-Based Composite PCMs

Random Single Graphene-Based Composite PCMs. Cao et al. (2019b) fabricated hexadecyl acrylate-grafted graphene (HDA-g-GN) via a solvent-free DA reaction. The resultant HDA-g-GN has an excellent electric conductivity of 219 S/m and thermal conductivity of 3.96 W/mK. To further improve the electrical conductivity of composite PCMs, Li et al. (2018) fabricated flexible graphene aerogel-directed smart fibers (ASFs) coated with hydrophobic fluorocarbon resin (Figures 6A and 6B). The resultant ASFs loading 53 wt% PEG exhibit a higher electric conductivity of 1,450 S/m, which is comparable with that of the graphene aerogel fiber (1,000 S/m) (Xu et al., 2012). When an appropriate working voltage is applied, the temperature of ASFs rapidly increases to the phase transition temperature plateau at 36°C. Moreover, the fracture strength of ASFs/PEG is 12.7 MPa, which is 70% higher than graphene/PEG because of the coherent core-shell

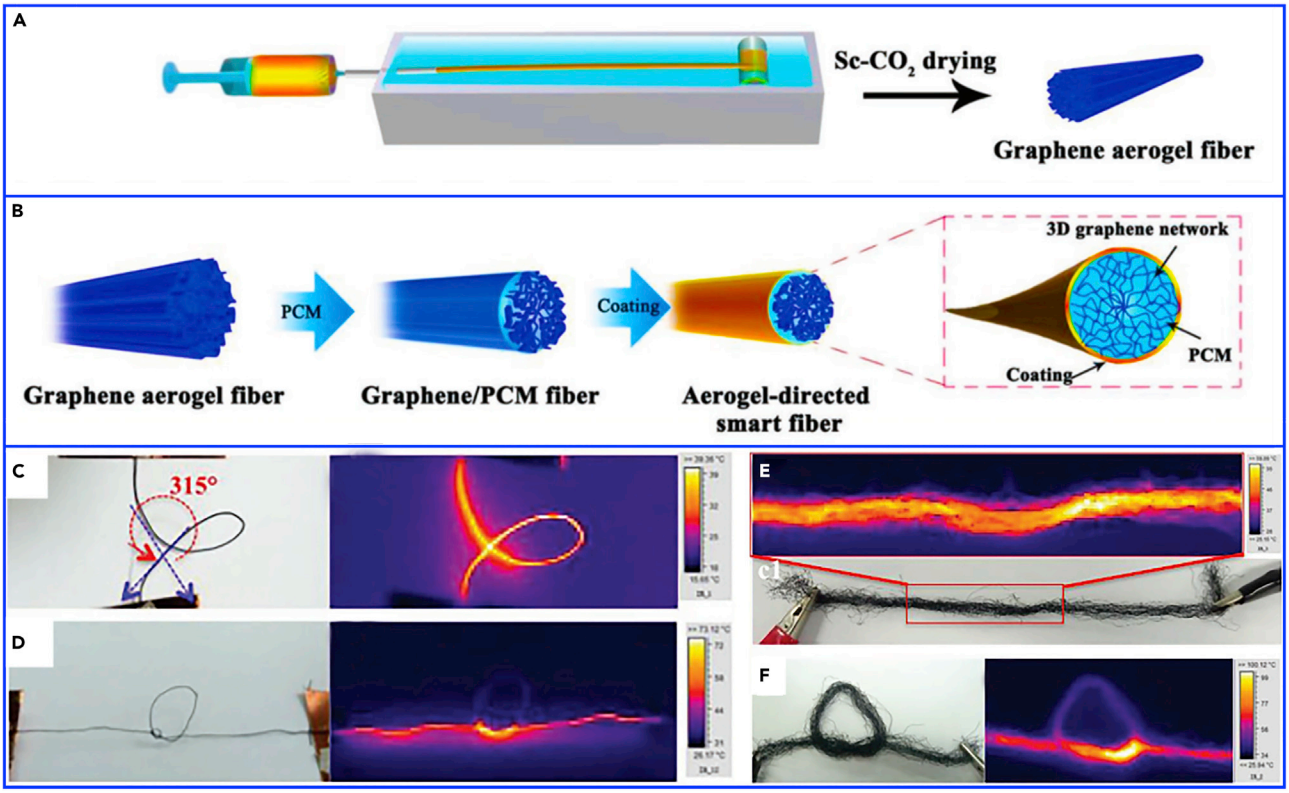

Figure 6. Single Graphene-Based Composite PCMs

(A and B) Preparation diagram of graphene aerogel fiber and graphene/PCMs smart fibers.

(C–F) Photographs and IR images of the ASFs by applying an input voltage. Adapted with permission from Li et al. (2018). Copyright 2018, Wiley-VCH.

structure of ASFs. It is noted that the temperature of ASFs in a bended "loop-like" shape remains steady at 40°C when the working voltage is 30 V, which is similar to the straight fiber at the same voltage, indicating the excellent strength and elasticity (Figure 6C). Furthermore, the temperature of the fiber knot is up to 72°C owing to the improved electrical and thermal conductivity of the fiber induced by the twisted graphene networks within the knots (Figure 6D). The temperature of the fiber knot is even higher than 100°C at 30 V because superhydrophobic coating can accelerate the electron transfer through the electronic tunneling (Figures 6E and 6F).

Array-Oriented Single Graphene-Based Composite PCMs. As previously mentioned, the array-oriented structure exhibits more potential to improve the electro-thermal conversion and storage of composite PCMs. Based on this design concept, Li et al. (2016) developed array-oriented graphene aerogel-based composite PCMs by processing the ordered graphene oxide liquid crystals, and then chemical reduction and annealing (Figures 7A and 7B). The anisotropic graphene aerogel (AN-GA) containing aligned honeycomb-like pores with less than 1 mm is shown in Figure 7C. After the encapsulation of paraffin, the thermal conductivity of AN-GA-paraffin reaches 1.2 W/mK in the radial direction (Figure 7D). The electric conductivity (258.7 S/m) of AN-GA-paraffin (94 wt%) still approaches that of pristine AN-GA (297 S/m), indicating that the effect of the introduced paraffin on disturbing the original graphene network is negligible. Therefore, the electro-thermal conversion efficiency of AN-GA-paraffin is up to 85.4% under a small voltage of 3.0 V (Figure 7E). In addition, AN-GA can significantly reduce the brittleness of paraffin owing to the excellent mechanical strength of AN-GA, and the corresponding composite PCMs can be compressed with nearly 5-fold strain without obvious damage.

Hybrid Graphene-Based Composite PCMs

Random Hybrid Graphene-Based Composite PCMs. In addition to the use of single graphene, graphene and other fillers are also considered as the hybrid supports for electro-thermal conversion of

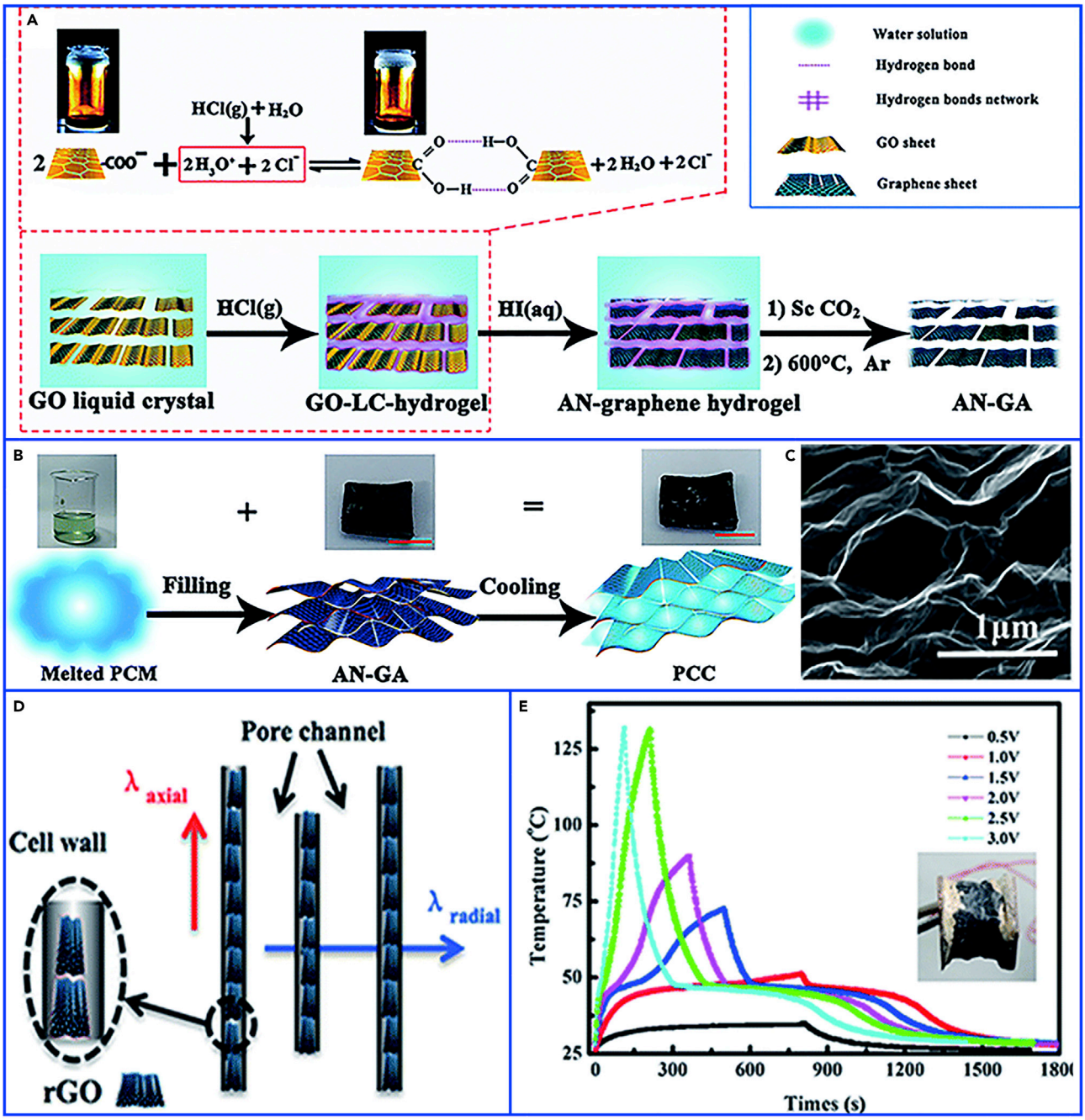

Figure 7. Single Graphene-Based Composite PCMs

(A) Preparation diagram of AN-GA based on vapor diffusion and the sol-gel process.

(B) Preparation diagram of paraffin/AN-GA composite PCMs.

(C) SEM image of AN-GA in the axial direction.

(D) Schematic illustration of the thermal conductivity in the axial and radial directions.

(E) Temperature evolution curves of paraffin/AN-GA composite PCMs under different voltages. Adapted with permission from Li et al. (2016). Copyright 2016, Royal Society of Chemistry.

composite PCMs. Xue et al. (2019) fabricated the hybrid aerogels composed of melamine foam (MF) and graphene oxide (GO)/graphene nanoplatelets (GNPs). After the carbonization of MF/GO/GNPs, paraffin was impregnated into the porous matrix (Figure 8). The resultant composite PCMs exhibit an increased phase change enthalpy of 161.7 J/g compared with pristine paraffin of 154.9 J/g owing to the interactions

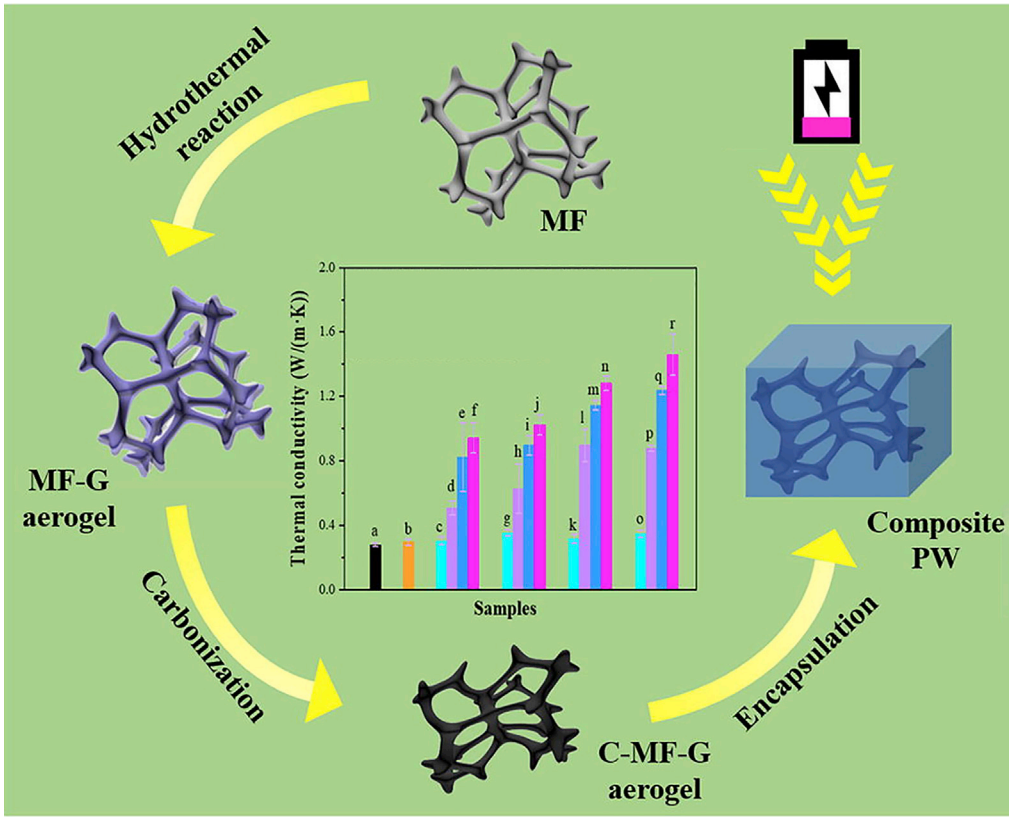

Figure 8. Random Hybrid Graphene-Based Composite PCMs

Schematic diagram and thermal conductivity of composite PCMs with rGO and GNPs covering on the carbonized MF framework. Adapted with permission from Xue et al. (2019). Copyright 2019, Elsevier.

between paraffin and MF/rGO/GNPs (Cui et al., 2012). Moreover, the thermal conductivity of composite PCMs is increased to 1.46 W/mK, which is approximatively 421% higher than that of pristine paraffin. The electrical conductivity of composite PCMs is also up to 2.79 S/cm when the content of rGO/GNPs is 4.89 wt% owing to the perfect and dense conductive network. As a result, the electro-thermal conversion efficiency is 62.5% at a small voltage (2.9 V) owing to the enhanced thermal conductivity and electrical conductivity of MF/rGO/GNPs.

In the study of Zhou et al. (2019), halloysite nanotubes (HNTs) were introduced for the preparation of HNTs-hybrid graphene aerogel (GA) (Figure 9A). HNTs can not only improve the reduction degree of GA but also increase the latent heat of composite PCMs owing to the heterogeneous nucleation effects (Yang et al., 2016, 2018). Thus, the phase change enthalpy of composite PCMs is improved to 103.3 J/g. More importantly, the electro-thermal energy conversion efficiency is up to 67.2% owing to the continuous 3D conductive network of GA. To further improve the thermal conductivity and electric-thermal conversion efficiency, Yang et al. (2020) prepared rGO/BN hybrid scaffold for the encapsulation of polyethylene glycol (PEG) via an ice-templated assembly strategy (Figure 9B). The resultant composite PCMs with 14.4 wt% BN exhibit a high thermal conductivity of 1.06 W/mK with an enhancement of 240% compared with pristine PEG owing to the synergistic effect of BN and rGO (Min et al., 2018; Yang et al., 2016). As a result, the electro-thermal energy conversion efficiency of composite PCMs is up to 87.9% at 7.0 V owing to the excellent electric conductivity of rGO/BN.

Array-Oriented Hybrid Graphene-Based Composite PCMs. As previously mentioned, the array-oriented structure exhibits more potential in electro-thermal conversion of PCMs. Based on this design concept, Wei et al. (2019) prepared microcrystalline cellulose (MCC)/GNPs aerogel with a highly array-oriented framework using a pre-refrigeration and freeze-drying method (Figure 10A). The introduction of GNPs facilitates the formation of porous anisotropic structure (Figures 10B and 10C). In the composite

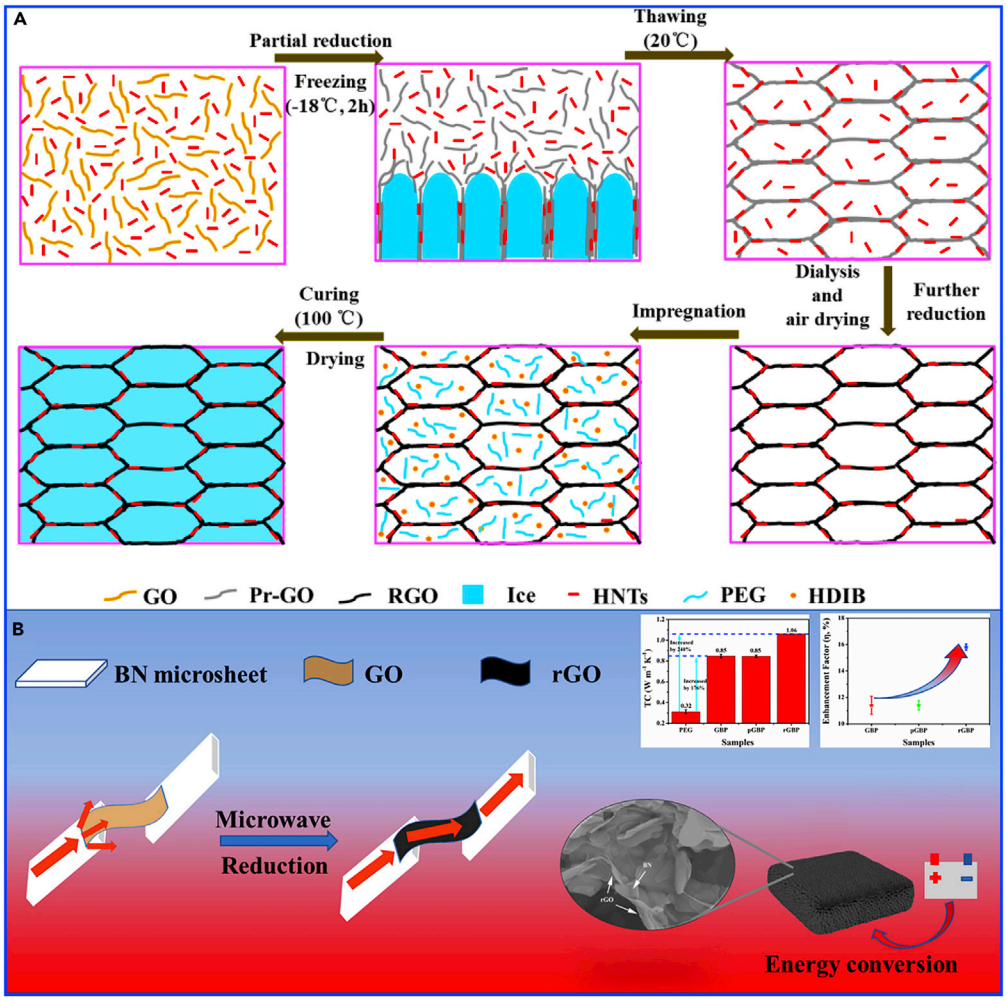

Figure 9. Random Hybrid Graphene-Based Composite PCMs

(A) Preparation diagram of composite PCMs. Adapted with permission from Zhou et al. (2019). Copyright 2019, Elsevier.

(B) Schematic illustration of the heat transfer model and electro-thermal conversion PCMs, and thermal properties of composite PCMs. Adapted with permission from Yang et al. (2020). Copyright 2020, Elsevier.

PCMs, the segregated anisotropic network of the stacked MCC/GNPs could enhance the electrical conductivity and thermal conductivity of composite PCMs (Figures 10D–10F). The thermal conductivity of composite PCMs with 1.51 wt% GNPs is up to 1.03 W/mK, which is 232% higher than that of the MCC/PEG without GNPs. Moreover, the temperature of composite PCMs increases from 26.7°C to 47.7°C within 15 min at a constant voltage, indicating the excellent electro-thermal energy conversion performance (Figure 10G). In addition, the 3D segregated anisotropic structure of MCC/GNPs can guarantee the homogeneous distribution of the Joule heat generated from electrical energy (Li et al., 2016; Wu et al., 2017).

Similarly, Xue et al. (2020) prepared array-oriented hybrid graphene-based electro-thermal composite PCMs via melamine foam (MF) and cellulose nanofiber (CNF) co-mediated assembly of GNPs (Figure 11A). The obtained hybrid graphene exhibits a parallel lamellar structure with an interlayer space of 50–70 μm and the paraffin can be well encapsulated into the interlayers (Figure 11B). The thermal conductivity of composite PCMs with 4.1 wt% GNPs is 1.42 W/mK with an increase of 407% compared with pristine paraffin owing to the array-oriented structure of the hybrid graphene aerogel. Hence, the enhanced thermal conductivity and excellent electric conductivity endow the composite PCMs an outstanding electro-thermal conversion capability. Wu et al. (2019a) infiltrated PEG into GNPs/CNF hybrid-coated MF (CG@MF) sponge for electro-thermal conversion (Figure 11C). The obtained composite PCMs exhibit a large phase change enthalpy

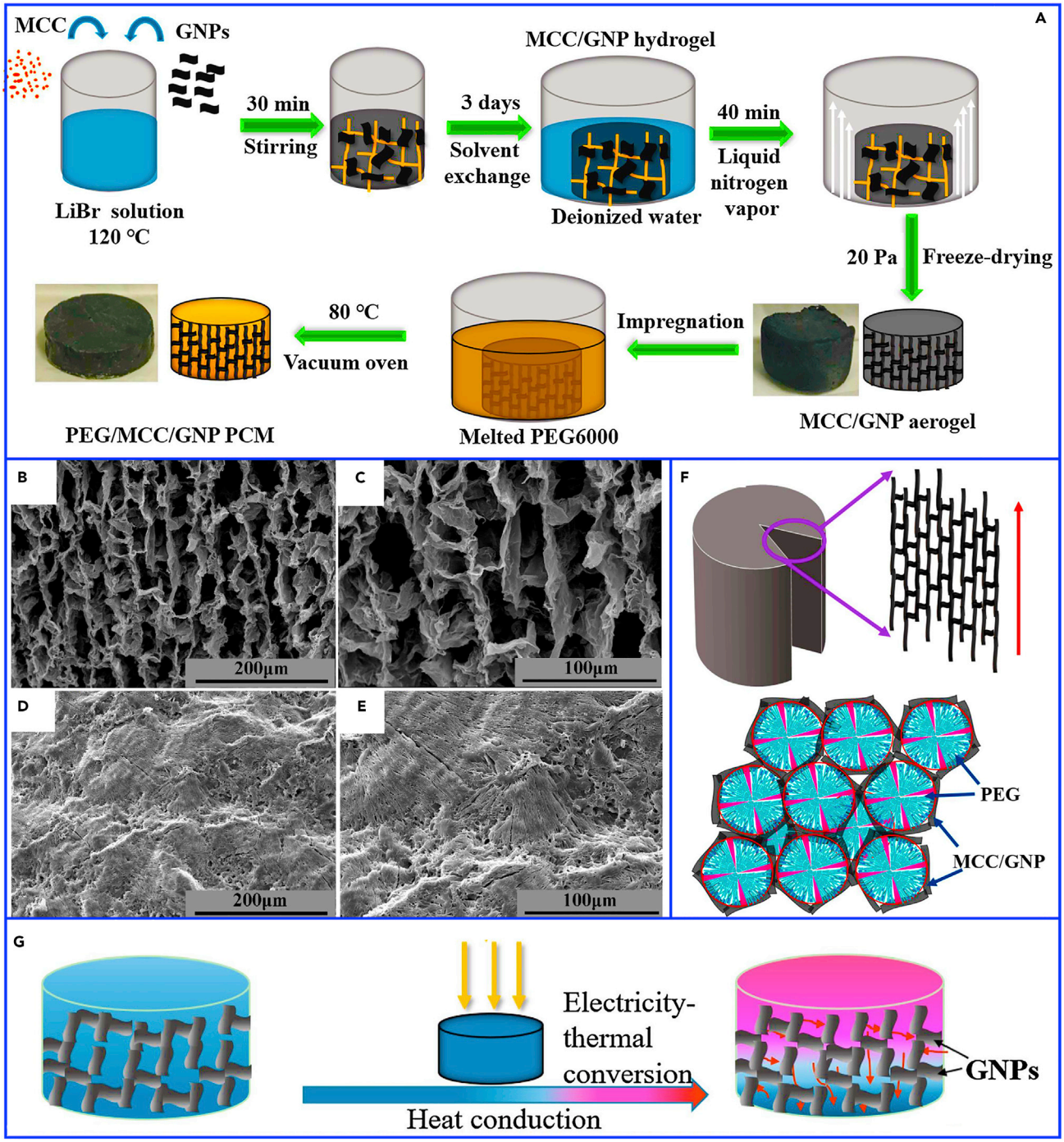

Figure 10. Array-Oriented Hybrid Graphene-Based Composite PCMs

(A) Preparation diagram of MCC/PEG/GNP composite PCMs.

(B and C) SEM images of MCC/GNP aerogel.

(D and E) SEM images of MCC/PEG/GNP.

(F) The corresponding schematic representation of the microstructure.

(G) Schematic representation of electro-thermal conversion and storage. Adapted with permission from Wei et al. (2019). Copyright 2019, Elsevier.

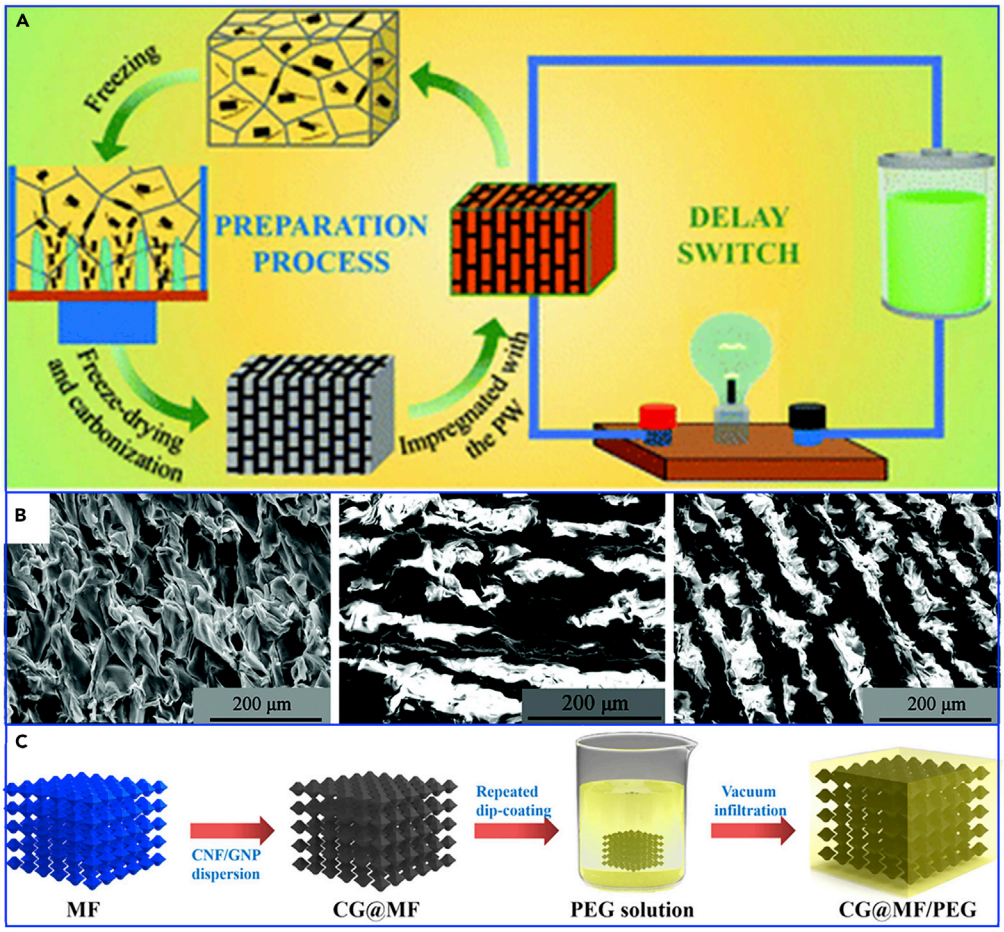

Figure 11. Array-Oriented Hybrid Graphene-Based Composite PCMs

(A) Schematic diagram of composite PCMs for electro-thermal conversion and storage.

(B) SEM images of paraffin and composite PCMs. Adapted with permission from Xue et al. (2020). Copyright 2020, Royal Society of Chemistry.

(C) Preparation diagram of CG@MF sponge and CG@MF/PEG composite PCMs. Adapted with permission from Wu et al. (2019a). Copyright 2019, American Chemical Society.

of 178.9 J/g. The thermal conductivity of CG@MF/PEG is 188.9% higher than that of MF/PEG owing to the introduction of single-layered graphene (Xue et al., 2019). More importantly, the electric conductivity of composite PCMs reaches 6.19 S/m, which is increased by 15 orders of magnitude compared with pristine PEG of 10^{-14} S/m. Consequently, composite PCMs exhibit an electro-thermal conversion efficiency of 66.13%.

In terms of hybrid graphene-based composite PCMs, the currently reported array-oriented graphene-based composite PCMs do not show the predicted advantages of electro-thermal conversion compared with random graphene-based composite PCMs. Therefore, array-oriented graphene-based composite PCMs with a more reasonable structure should be designed rationally to pursue higher electro-thermal conversion efficiency.

Biomass-Derived Carbon-Based Composite PCMs for Electro-Thermal Conversion and Storage

The brittleness is also an issue worth addressing in addition to low thermal conductivity and poor electro-thermal conversion ability of PCMs. As stated earlier, several studies have confirmed the high electro-thermal conversion efficiency of CNTs and graphene-based composite PCMs at a low voltage. However, most of these electro-thermal conversion composite PCMs possess rigid structure and lack enough flexibility, which may cause poor installation effect because of the insufficient surface contact. In terms of brittleness issue, the integration of PCMs in electrospun polymer and fibers supporting materials is a feasible strategy

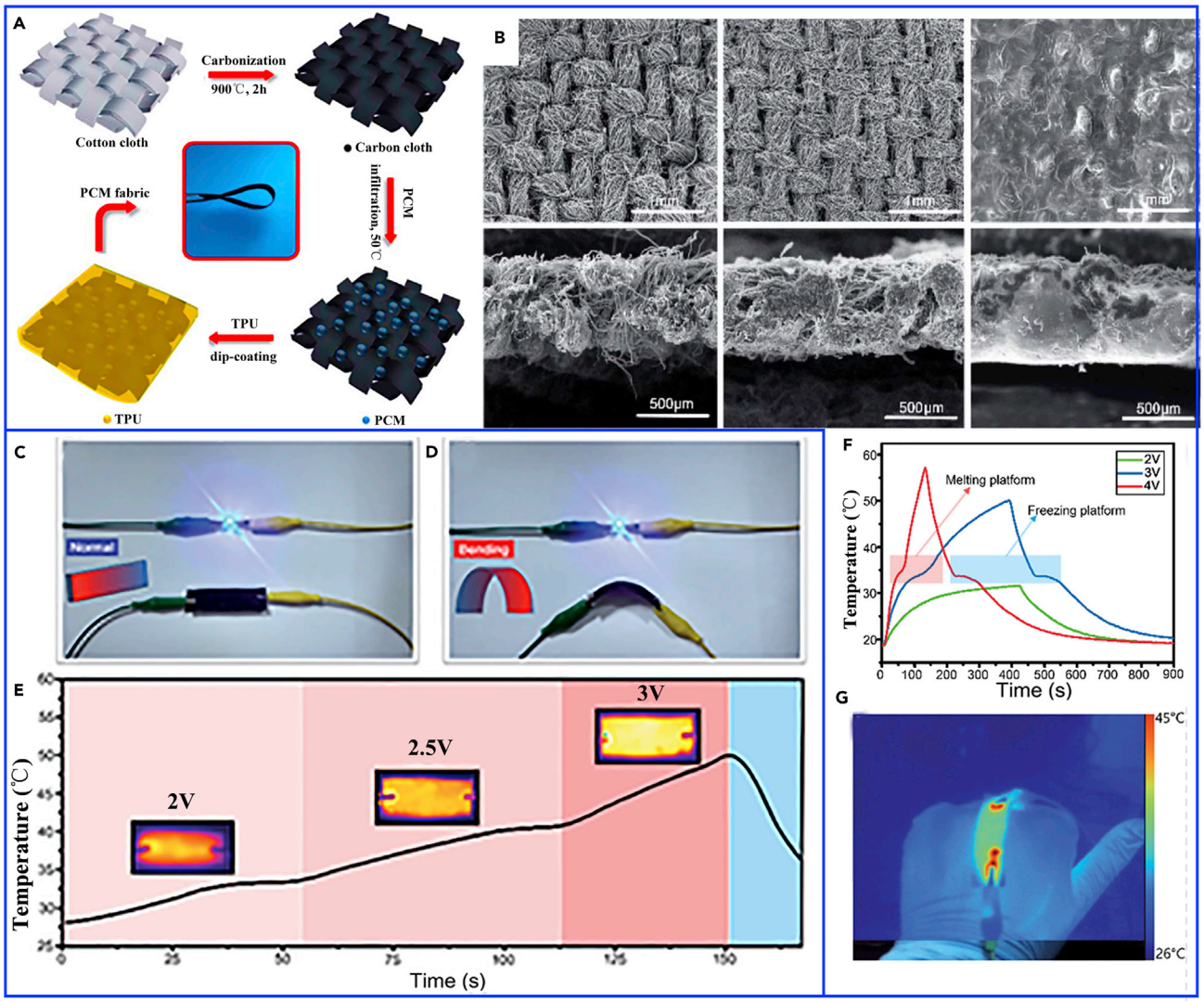

Figure 12. Biomass-Derived Carbon-Based Composite PCMs

(A) Preparation diagram of composite PCMs.

(B) SEM images of carbon cloth and composite PCMs.

(C and D) LED lit by composite PCMs in normal and deformed states.

(E) Temperature evolution curve of composite PCMs under a stepwise voltage.

(F) Temperature evolution curve of composite PCMs under different voltages.

(G) Composite PCMs attached to a hand functioning as a flexible heater. Adapted with permission from Umair et al. (2019b). Copyright 2019, Royal Society of Chemistry.

to develop flexible composite PCMs. However, this electrospinning strategy has two major deficiencies: insufficient mechanical strength and low encapsulation efficiency of PCMs.

The flexibility of most reported flexible composite PCMs only emerges in the melted state of PCMs. In contrast, the flexibility would drop sharply or disappear completely in the solidified state of PCMs. To develop real flexible electro-thermal conversion composite PCMs in both melted and solidified states of PCMs, Umair et al. (2019b) proposed a facile and low-cost strategy that intelligently combines the functions of inorganic and organic materials with PCMs. The prepared carbon cloth (CC) after carbonization of a cotton cloth at 900°C contains hollow fibers as a flexible conductive skeleton. After infiltrating paraffin, an efficient PCMs-based electro-thermal conversion system (Figure 12A) is constructed through the conductive paths of highly graphitized and well-aligned CC. Moreover, the coated thermoplastic polyurethane (TPU)

interpenetrating layer on the surfaces of CC/paraffin simultaneously improve the mechanical strength and flexibility of composite PCMs (Figure 12B). Therefore, CC/paraffin/TPU composite PCMs show the satisfactory bending and twisting deformation below and above the phase change temperature. Additionally, the electro-thermal conversion efficiency of CC/paraffin/TPU composite PCMs is up to 67.39% at 4.0 V owing to high electrical conductivity (374 S/m) of highly graphitized and well-aligned CC (Figures 12C–12F). This design strategy of flexible electrothermal composite PCMs provides insightful contributions to the development of intelligent temperature regulation devices (Figure 12G).

Although the aforementioned CNTs and graphene-based composite PCMs have shown superior electro-thermal conversion capability, the complex equipment or expensive and harmful precursors involved in the preparation of CNTs and graphene have dramatically hindered their large-scale production. Therefore, Li et al. (2014) proposed a facile, environmentally friendly and economical strategy to prepare carbonaceous materials on a large scale using the sustainable and renewable biomass materials. The various melons (such as watermelon, winter melon, and pumpkin) containing more than 90% water are used to prepare lightweight, highly thermally and electrically conductive 3D carbon aerogels using a hydrothermal carbonization and post pyrolysis method (Figure 13A). The obtained carbon aerogels exhibit an ultrahigh porosity of more than 95% (Figure 13B), which is slightly smaller than that of graphene aerogels (99.5%–98%) and CNTs aerogels (99.5%–99%) (Chen et al., 2011, 2012; Gui et al., 2010; Sudeep et al., 2013; Wu et al., 2013; Zhong et al., 2013). After infiltrating paraffin, the resultant composite PCMs exhibit phase change enthalpy of 115.2 J/g and electro-thermal conversion efficiency of 71.4% at 15 V owing to the moderate electrical resistance of 3.4 S/m.

To further improve the electro-thermal conversion efficiency of biomass-derived carbon-based composite PCMs, Umair et al. (2020) prepared 3D hollow carbon fiber (HCF) network scaffold via an alkaline treatment and subsequent pyrolysis of raw cotton (Figure 13C). After the alkali treatment, the specific surface area, pore volume, and pore size distribution of HCF are significantly improved. Importantly, 3D HCF exhibits highly interconnected thermally and electrically conductive paths in the HCF/paraffin composite PCMs. The phase change enthalpy of composite PCMs is as high as 182.22 J/g when the loading paraffin is 85 wt%. The corresponding electrical conductivity is 19.6 S/m, whereas that of pristine paraffin is around 10^{-14} S/m, indicating that the insulating nature of paraffin is overcome by the electrically conductive paths of HCF. As a result, the electro-thermal conversion efficiency (Figures 13D–13F) of HCF-based composite PCMs is up to 81.1% at 3 V owing to the efficient Joule heating effect provided by the long conductive paths of HCF.

Compared with the aforementioned CNTs and graphene-based composite PCMs for electro-thermal conversion, porous carbon derived from biomass sources is considered to be more promising owing to their sustainable raw materials, simple preparation process, large-scale carbon production, and impressive thermophysical properties. However, the electro-thermal conversion efficiency of current biomass-derived carbon-based composite PCMs is relatively low, which needs to be further improved.

Other Composite PCMs for Electro-Thermal Conversion and Storage

MXene, layered 2D transition metal carbides/nitrides, has high specific surface area, large layer spacing, rich hydrophilic groups, and excellent electrical and thermal conductive properties, thus showing great potential in the field of PCMs for thermal energy storage. However, up to now, there are still few reports concerning MXene-based composite PCMs. Theoretically, high specific surface area and rich hydrophilic groups of MXene would create strong hydrogen bonding interactions and adsorption force for the water-soluble PCMs molecules. On this basis, Lu et al. (2019) developed electro-driven water-soluble PEG/MXene (Figure 14A) composite PCMs with enhanced electrical conductivity and thermal conductivity via a simple vacuum impregnation. The polarizing microscope (POM) results indicate that 2D MXene nanosheets serve as heterogeneous crystal nuclei to enhance the crystallization of PEG molecules (Figures 14B–14D). Consequently, the melting and freezing enthalpies of PEG/MXene composite PCMs are up to 131.2 and 129.5 J/g, respectively. The corresponding electrical conductivity and thermal conductivity are 10.41 S/m (pristine PEG is 10^{-11} S/m) and 2.05 W/mK (pristine PEG is 0.29 W/mK), respectively. Therefore, PEG/MXene exhibits an excellent electro-thermal conversion and storage performance owing to the interconnected MXene.

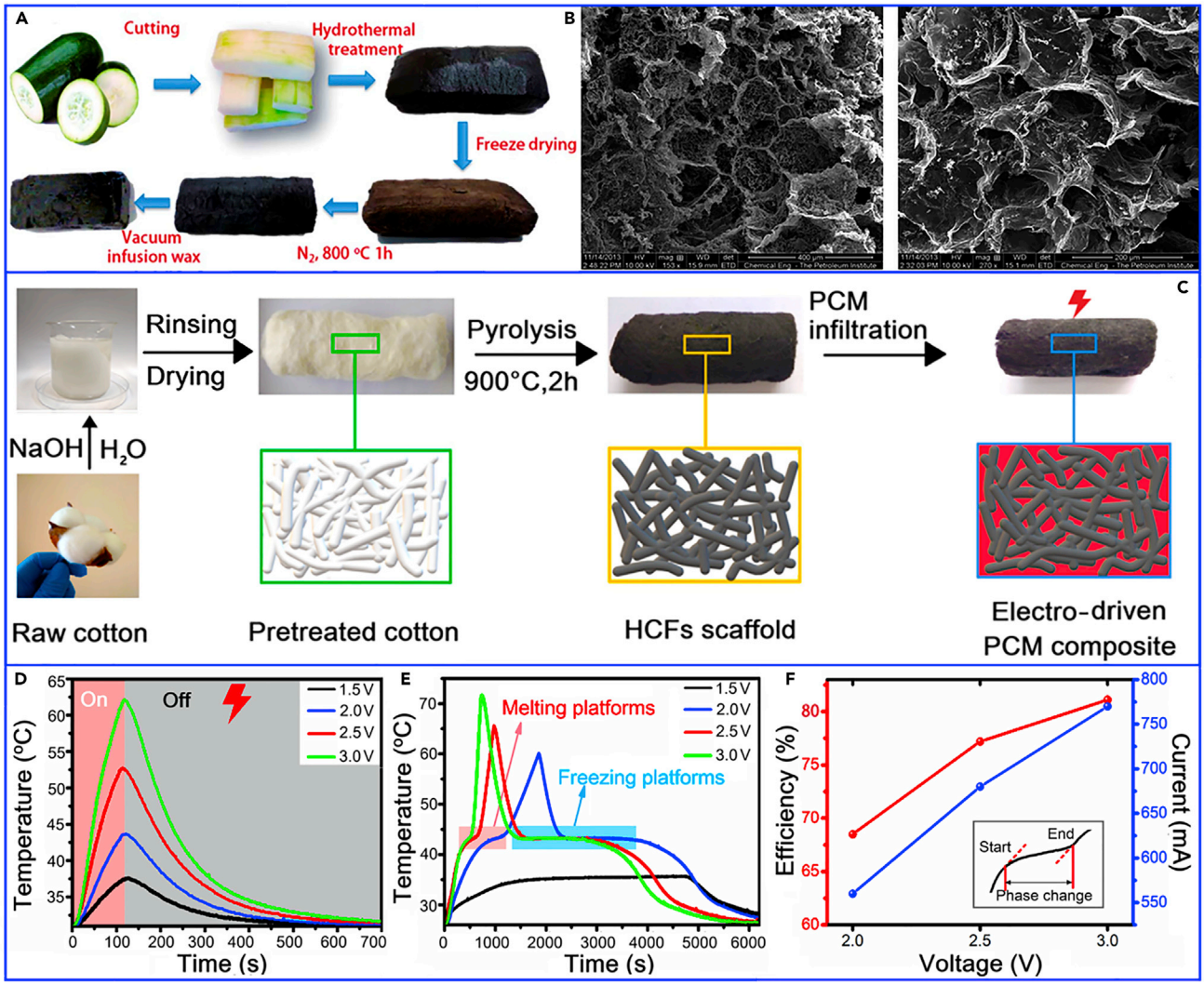

Figure 13. Biomass-Derived Carbon-Based Composite PCMs

(A) Preparation diagram of carbon aerogels and composite PCMs.

(B) SEM images of carbon aerogels from watermelon and pumpkin. Adapted with permission from Li et al. (2014). Copyright 2014, Royal Society of Chemistry.

(C) Preparation diagram of composite PCMs.

(D) Temperature evolution curves of an empty HCF under different voltages.

(E) Temperature evolution curves of composite PCMs under different voltages.

(F) Electro-thermal conversion efficiencies of composite PCMs under different voltages. Adapted with permission from Umair et al. (2020). Copyright 2020, American Chemical Society.

Our group (Li et al., 2020a) fabricated CNTs@porous carbon-based electrothermal PCMs through a gradient carbonization of zeolitic imidazolate framework@metal-organic frameworks (ZIF@MOFs) (Figure 14E). During the carbonization process, MOFs shells were decomposed to form porous carbon (PC) shells. ZIF was decomposed to form Co clusters, which serve as catalyst to boost the formation of CNTs. The obtained CNTs penetrated highly graphitized porous carbon enables efficient encapsulation of PCMs and electro-thermal conversion. The critical triggering voltage is as low as 1.1 V with a high electro-thermal conversion efficiency of 94.5%. Zhang et al. (2018) prepared PEG·$CaCl_2$-based electro-thermal conversion PCMs via ligand replacement and introducing acetylene black conductive network. The acetylene black fillers not only enhance the electrical/thermal conductivity but also boost the mechanical properties of composite PCMs at high temperature. The electrical resistivity of PEG·$CaCl_2$-based composite PCMs is reduced from 10^7–10^{12} to 0.3 Ω·m, and the thermal conductivity is improved by 300% when acetylene black is 20 wt%. Therefore, electro-thermal conversion can be triggered by a low voltage of 1.8 V

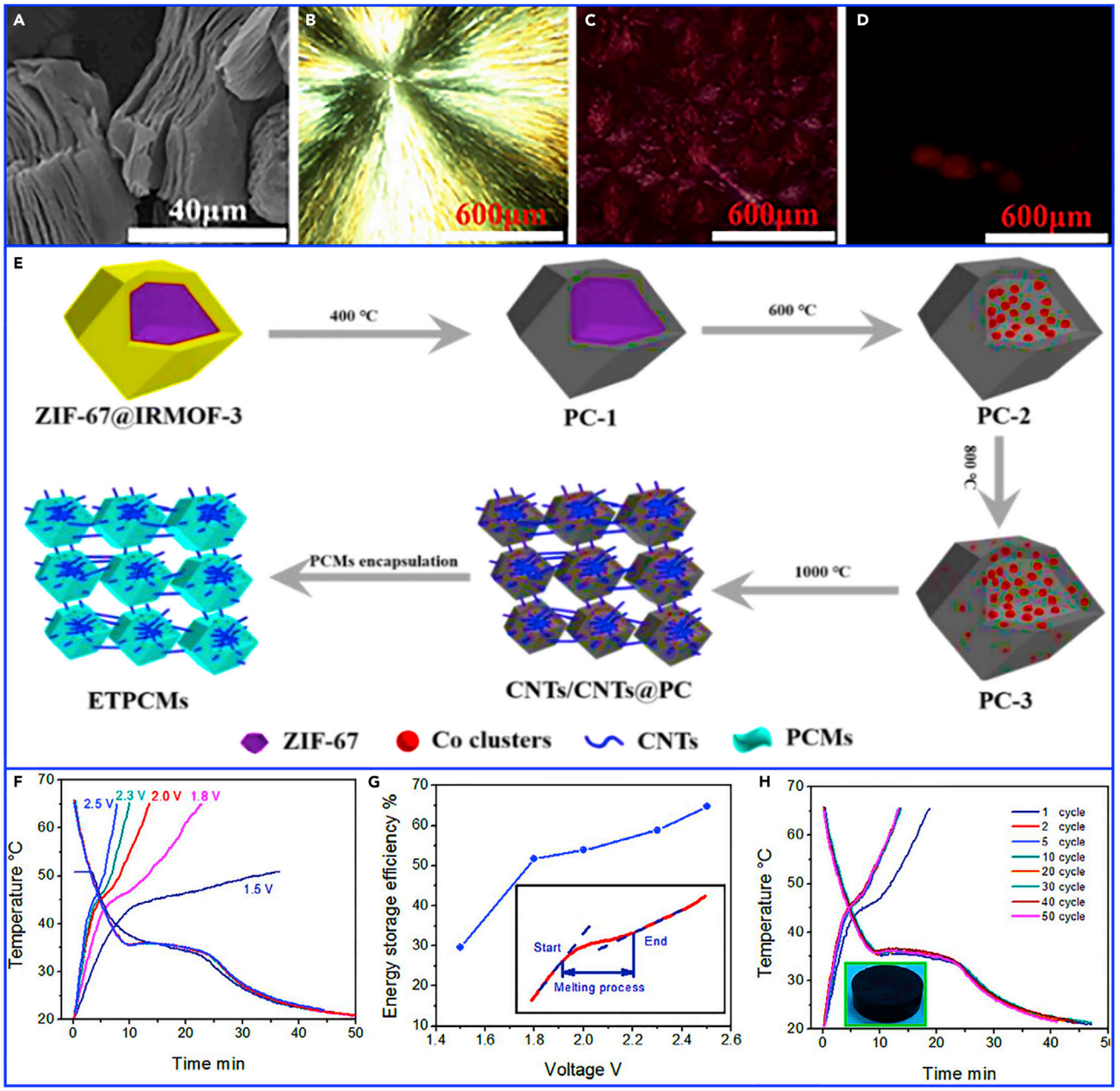

Figure 14. MXene, MOFs-Derived Carbon, and Acetylene Black-Based Composite PCMs

(A) SEM image of multilayered MXene.

(B–D) POM images of pristine PEG, PEG@MXene at room temperature, PEG@MXene at 80°C. Adapted with permission from Lu et al. (2019). Copyright 2019, Elsevier.

(E) Preparation diagram of MOFs-derived carbon-based composite PCMs. Adapted with permission from Li et al., 2020a. Copyright 2020, Wiley-VCH.

(F) Temperature evolution curves of composite PCMs under different voltages.

(G) Electro-thermal conversion efficiencies of composite PCMs under different voltages.

(H) Temperature evolution curves of composite PCMs under 2.0 V for 50 cycles. Adapted with permission from Zhang et al. (2018). Copyright 2018, Elsevier.

(Figure 14F). The maximum electro-thermal conversion efficiency is 64.7% at 2.5 V (Figure 14G). Additionally, composite PCMs show the superior electro-thermal conversion stability (Figure 14H).

In addition to the aforementioned advanced MXene and MOFs-derived carbon for electro-thermal conversion, the traditional expanded graphite (EG) and graphite are also considered as the supporting materials

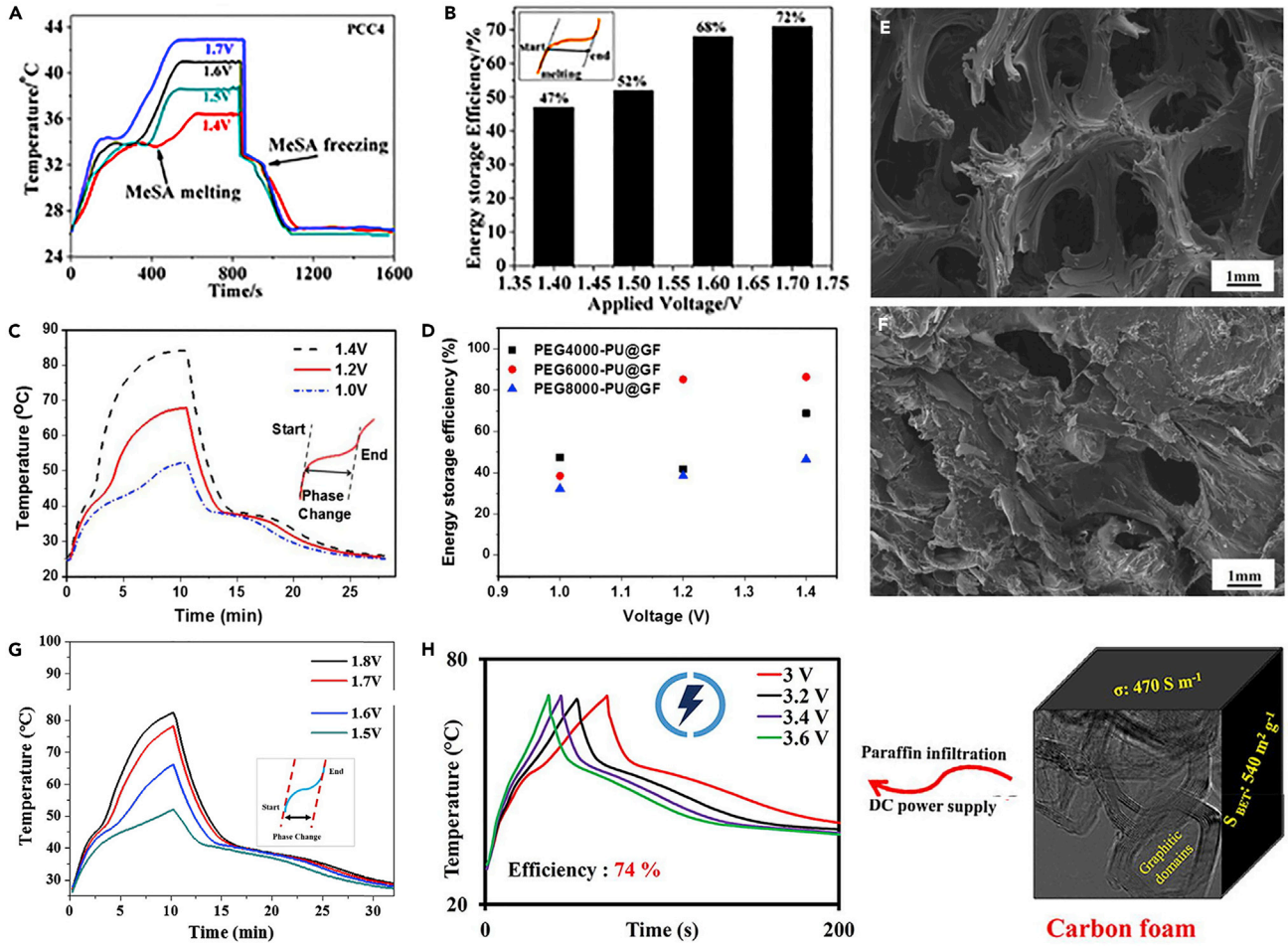

Figure 15. Other Carbon-Based Composite PCMs

(A) Temperature evolution curves of composite PCMs under different voltages.

(B) Electro-thermal conversion efficiencies of composite PCMs under different voltages. Adapted with permission from Tabassum et al. (2015). Copyright 2015, Elsevier.

(C) Temperature evolution curves of composite PCMs under different voltages.

(D) Electro-thermal conversion efficiencies of composite PCMs under different voltages. Adapted with permission from Chen et al. (2015). Copyright 2015, Elsevier.

(E and F) SEM image of graphite foam and composite PCMs.

(G) Temperature evolution curves of composite PCMs under different voltages. Adapted with permission from Wu et al. (2017). Copyright 2017, Elsevier.

(H) Temperature evolution curves of composite PCMs under different voltages. Adapted with permission from Maleki et al. (2019). Copyright 2019, Elsevier.

to trigger the electro-thermal conversion of PCMs. Tabassum et al. (2015) developed multifunctional methyl stearate (MeSA)/EG-based composite PCMs with an electro-thermal conversion efficiency of 72% at 1.7 V. The smallest triggering voltage of the electro-thermal conversion is as low as 1.4 V (Figures 15A and 15B) owing to high electrical and thermal conductivity of EG. In addition, the added nano-organophilic montmorillonite and ammonium polyphosphate endow PCMs flame retardant function. Graphite foam (GF) can also encapsulate polyurethane through *in situ* polymerization of PEG for electro-thermal conversion (Chen et al., 2015). The thermal conductivity of composite PCMs is dramatically increased to 3.5 W/mK (12 times enhancement to pristine PEG) and the corresponding resistance is very small (0.86–1.00 Ω). These excellent electrical and thermal conductivities contribute a high electro-thermal conversion efficiency (exceeding 80% at 1.2 or 1.4 V) (Figures 15C and 15D). Wu et al. (2017) further prepared polyurethane/pitch-based graphite foam (PGF) (Figures 15E and 15F) with a superhigh thermal conductivity of 10.86 W/mK, which is 43 times that of the polyurethane. Hence, highly efficient electro-thermal conversion (85%, 1.8 V) is obtained (Figure 15G).

Highly graphitized carbon foam also contributes a possibility for electro-thermal conversion of PCMs. In this regard, Maleki et al. (2019) prepared highly graphitized 3D interconnected hierarchical carbon foam by carbonizing poly(acrylonitrile-co-divinylbenzene) P(AN-co-DVB) polyHIPE foam at 900°C. The prepared carbon foam exhibits a high specific surface area (540 m^2/g), large pore volume (0.4 cm^3/g), semi-ordered nanoporosity, and high electrical conductivity (470 S/m). Generally, larger pore volume, ordered pore, and 3D interconnected porous structure of carbon foam are beneficial to reach a higher latent heat. Consequently, the latent heat of carbon foam/PEG composite PCMs is up to 163.9 J/g. More importantly, this continuous highly electrically conductive network of carbon foam contributes a high electro-thermal conversion efficiency (85%, 3.6 V) of composite PCMs (Figure 15H). In addition, composite PCMs demonstrate the outstanding reversible thermal/chemical stability after 200 heating/cooling cycles.

In addition to non-metallic materials, Zhang et al. (2019b) synthesized hierarchical silver nanowire (AgNW) aerogel with anisotropic electrical and thermal properties using a bidirectional freeze-casting method. The AgNW ribbons are connected by AgNW bridges, thus obtaining an ultrahigh porosity of ~99.7%. After infiltrating paraffin, the resultant composite PCMs exhibit a thermal conductivity of 0.35 W/mK and an electrical conductivity of ~0.6 S/cm. The electronic conduction pathways are completely attributed to the AgNW network in composite PCMs. To further improve the thermal and electrical conductivity of metal aerogel-based composite PCMs, Zhang et al. (2019a) fabricated copper nanowire (CuNW) aerogel for the encapsulation of PCMs. The resultant CuNW aerogel-paraffin composite PCMs integrate excellent thermal conductivity (0.48 W/mK) and electrical conductivity (6.85 S/m). These highly conductive nano metal-based composite PCMs show promising application potential in the field of electro-thermal conversion.

However, the corresponding researches concerning advanced MXene, MOFs-derived carbon, and nano metal aerogel-based composite PCMs for electro-thermal conversion are still in infancy, which need more research and improvement in the future.

CONCLUSIONS AND PERSPECTIVES

Advanced functional electro-thermal conversion PCMs have widened the application scope of PCMs. Herein, we provide a comprehensive review on the significant advances in different electro-thermal conversion PCMs, mainly including CNTs, graphene, biomass-derived carbon, MOFs-derived carbon, graphite, highly graphitized carbon, and MXene-based composite PCMs. To trigger the electro-thermal conversion and storage of pristine PCMs, electrically conductive supporting materials are introduced into PCMs to prepare composite PCMs for electro-thermal conversion and storage. The constructed conductive paths from functional fillers are influenced by their pore structure, spatial arrangement, degree of orientation, and synergistic effect of hybrid fillers. These influencing factors play an important role in reducing the systematic electrical and thermal resistance to enhance the electro-thermal conversion of composite PCMs. Comparatively, highly array-oriented and synergistic hybrid fillers are more conducive to improving the electro-thermal conversion of composite PCMs. In addition, the summarized electro-thermal conversion mechanisms and the relationships between structure design and electrothermal properties can make it easy for readers to deeply understand the theoretical and experimental basis and can provide constructive guidance for the design and development of high-performance electro-thermal conversion PCMs.

Although electro-thermal conversion PCMs have made great progress, several critical issues and research directions deserve further investigation as follows. (1) Current electro-thermal conversion PCMs are difficult to achieve a good balance of small driving voltage and high conversion efficiency. Therefore, high-performance electro-thermal conversion PCMs with small driving voltage and high conversion efficiency will be the focus of future research and development. (2) Current electro-thermal supporting materials are mainly carbonaceous materials; more other advanced electrically triggered materials need further development, such as MXene and boron nitride. (3) MOFs-derived carbon-based composite PCMs are a kind of very promising candidate for electro-thermal conversion owing to their adjustable pore structure, ultra-high specific surface area, and porosity. However, the relevant researches are still in infancy. (4) Most electro-thermal conversion PCMs are concentrated on the structural analysis scale, lacking an in-depth understanding from the perspective of electron collision mechanism. (5) The fundamental micro-process of electro-thermal conversion is still unclear. Advanced visualization techniques are needed to achieve real-time dynamic observation of electro-thermal conversion of composite PCMs. (6) The current calculation method for electro-thermal conversion efficiency needs further optimization because it does not consider the heat loss of the test samples exposed to the external environment. (7) The relationships

between structure/compositions and corresponding electrothermal properties remain to be better clarified for further optimization of electro-thermal conversion PCMs. (8) After all, there is still a long way to go before these electro-thermal conversion PCMs realize their scale application. With continuous research efforts, more objective insights can provide more information and trade off the fundamental design and engineering application.

ACKNOWLEDGMENTS

This work was financially supported by the National Natural Science Foundation of China (No. 51436001, 51902025 and 51702013), the Fundamental Research Funds for the Central Universities (2019NTST29), and the China Postdoctoral Science Foundation (No. 2019M660520).

AUTHOR CONTRIBUTIONS

Conceptualization: X.C. and G.W.; Visualization: X.C.; Writing – Original Draft: X.C. and Z.T.; Writing – Review & Editing: X.C. and G.W.; Copyright: S.C. and H.G.; Funding Acquisition: X.C., H.G., and G.W.; Supervision: X.C. and G.W.

REFERENCES

Aftab, W., Huang, X., Wu, W., Liang, Z., Mahmood, A., and Zou, R. (2018). Nanoconfined phase change materials for thermal energy applications. Energy Environ. Sci. *11*, 1392–1424.

Aftab, W., Mahmood, A., Guo, W., Yousaf, M., Tabassum, H., Huang, X., Liang, Z., Cao, A., and Zou, R. (2019). Polyurethane-based flexible and conductive phase change composites for energy conversion and storage. Energy Storage Mater. *20*, 401–409.

Allahbakhsh, A., and Arjmand, M. (2019). Graphene-based phase change composites for energy harvesting and storage: state of the art and future prospects. Carbon *148*, 441–480.

Arivazhagan, R., Geetha, N., Sivasamy, P., Kumaran, P., Gnanamithra, M.K., Sankar, S., Loganathan, G.B., and Arivarasan, A. (2020). Review on performance assessment of phase change materials in buildings for thermal management through passive approach. Mater. Today Proc. *22*, 419–431.

Avery, A.D., Zhou, B.H., Lee, J., Lee, E.-S., Miller, E.M., Ihly, R., Wesenberg, D., Mistry, K.S., Guillot, S.L., Zink, B.L., et al. (2016). Tailored semiconducting carbon nanotube networks with enhanced thermoelectric properties. Nat. Energy *1*, 16033.

Back, H., Kim, G., Kim, H., Nam, C.-Y., Kim, J., Kim, Y.R., Kim, T., Park, B., Durrant, J.R., and Lee, K. (2020). Highly stable inverted methylammonium lead tri-iodide perovskite solar cells achieved by surface re-crystallization. Energy Environ. Sci. *13*, 840–847.

Balandin, A.A. (2011). Thermal properties of graphene and nanostructured carbon materials. Nat. Mater. *10*, 569–581.

Bertoluzzi, L., Boyd, C.C., Rolston, N., Xu, J., Prasanna, R., O'Regan, B.C., and McGehee, M.D. (2020). Mobile ion concentration measurement and open-access band diagram simulation platform for halide perovskite solar cells. Joule *4*, 109–127.

Cao, R., Chen, S., Wang, Y., Han, N., Liu, H., and Zhang, X. (2019a). Functionalized carbon nanotubes as phase change materials with enhanced thermal, electrical conductivity, light-to-thermal, and electro-to-thermal performances. Carbon *149*, 263–272.

Cao, R., Liu, H., Chen, S., Pei, D., Miao, J., and Zhang, X. (2017). Fabrication and properties of graphene oxide-grafted-poly (hexadecyl acrylate) as a solid-solid phase change material. Compos. Sci. Technol. *149*, 262–268.

Cao, R., Wang, Y., Chen, S., Han, N., Liu, H., and Zhang, X. (2019b). Multiresponsive shape-stabilized hexadecyl acrylate-grafted graphene as a phase change material with enhanced thermal and electrical conductivities. ACS Appl. Mater. Interfaces *11*, 8982–8991.

Cao, S., Piao, L., and Chen, X. (2020). Emerging photocatalysts for hydrogen evolution. Trends Chem. *2*, 57–70.

Chen, L., Zou, R., Xia, W., Liu, Z., Shang, Y., Zhu, J., Wang, Y., Lin, J., Xia, D., and Cao, A. (2012). Electro-and photodriven phase change composites based on wax-infiltrated carbon nanotube sponges. ACS Nano *6*, 10884–10892.

Chen, R., Yao, R., Xia, W., and Zou, R. (2015). Electro/photo to heat conversion system based on polyurethane embedded graphite foam. Appl. Energy *152*, 183–188.

Chen, X., Gao, H., Hai, G., Jia, D., Xing, L., Chen, S., Cheng, P., Han, M., Dong, W., and Wang, G. (2020). Carbon nanotube bundles assembled flexible hierarchical framework based phase change material composites for thermal energy harvesting and thermotherapy. Energy Storage Mater. *26*, 129–137.

Chen, X., Gao, H., Xing, L., Dong, W., Li, A., Cheng, P., Liu, P., and Wang, G. (2019a). Nanoconfinement effects of N-doped hierarchical carbon on thermal behaviors of organic phase change materials. Energy Storage Mater. *18*, 280–288.

Chen, X., Gao, H., Yang, M., Dong, W., Huang, X., Li, A., Dong, C., and Wang, G. (2018). Highly graphitized 3D network carbon for shape-stabilized composite PCMs with superior thermal energy harvesting. Nano Energy *49*, 86–94.

Chen, X., Gao, H., Yang, M., Xing, L., Dong, W., Li, A., Zheng, H., and Wang, G. (2019b). Smart integration of carbon quantum dots in metal-organic frameworks for fluorescence-functionalized phase change materials. Energy Storage Mater. *18*, 349–355.

Chen, Z., Ren, W., Gao, L., Liu, B., Pei, S., and Cheng, H.-M. (2011). Three-dimensional flexible and conductive interconnected graphene networks grown by chemical vapour deposition. Nat. Mater. *10*, 424.

Cheng, P., Gao, H., Chen, X., Chen, Y., Han, M., Xing, L., Liu, P., and Wang, G. (2020). Flexible monolithic phase change material based on carbon nanotubes/chitosan/poly (vinyl alcohol). Chem. Eng. J. *397*, 125330.

Cui, Y., Xu, H., Yue, Y., Guo, Z., Yu, J., Chen, Z., Gao, J., Yang, Y., Qian, G., and Chen, B. (2012). A luminescent mixed-lanthanide metal–organic framework thermometer. J. Am. Chem. Soc. *134*, 3979–3982.

Drissi, S., Ling, T.-C., Mo, K.H., and Eddhahak, A. (2019). A review of microencapsulated and composite phase change materials: alteration of strength and thermal properties of cement-based materials. Renew. Sustain. Energy Rev. *110*, 467–484.

Fei, J., Duan, X., Luo, L., Zhang, C., Qi, Y., Li, H., Feng, Y., and Huang, J. (2018). Grafting methyl acrylic onto carbon fiber via Diels-Alder reaction for excellent mechanical and tribological properties of phenolic composites. Appl. Surf. Sci. *433*, 349–357.

Feng, D., Feng, Y., Qiu, L., Li, P., Zang, Y., Zou, H., Yu, Z., and Zhang, X. (2019). Review on nanoporous composite phase change materials: fabrication, characterization, enhancement and molecular simulation. Renew. Sustain. Energy Rev. *109*, 578–605.

Göhl, D., Garg, A., Paciok, P., Mayrhofer, K.J., Heggen, M., Shao-Horn, Y., Dunin-Borkowski, R.E., Román-Leshkov, Y., and Ledendecker, M. (2020). Engineering stable electrocatalysts by synergistic stabilization between carbide cores and Pt shells. Nat. Mater. *19*, 287–291.

Gao, C., Low, J., Long, R., Kong, T., Zhu, J., and Xiong, Y. (2020). Heterogeneous single-atom photocatalysts: fundamentals and applications.

Chem. Rev. https://doi.org/10.1021/acs.chemrev.9b00840.

Gao, H., Wang, J., Chen, X., Wang, G., Huang, X., Li, A., and Dong, W. (2018). Nanoconfinement effects on thermal properties of nanoporous shape-stabilized composite PCMs: a review. Nano Energy *53*, 769–797.

Gui, X., Wei, J., Wang, K., Cao, A., Zhu, H., Jia, Y., Shu, Q., and Wu, D. (2010). Carbon nanotube sponges. Adv. Mater. *22*, 617–621.

Gulotty, R., Castellino, M., Jagdale, P., Tagliaferro, A., and Balandin, A.A. (2013). Effects of functionalization on thermal properties of single-wall and multi-wall carbon nanotube–polymer nanocomposites. ACS Nano *7*, 5114–5121.

Guo, X., Liu, C., Li, N., Zhang, S., and Wang, Z. (2018). Electrothermal conversion phase change composites: the case of polyethylene glycol infiltrated graphene oxide/carbon nanotube networks. Ind. Eng. Chem. Res. *57*, 15697–15702.

Hosaka, T., Kubota, K., Hameed, A.S., and Komaba, S. (2020). Research development on K-ion batteries. Chem. Rev. https://doi.org/10.1021/acs.chemrev.9b00463.

Huang, X., Chen, X., Li, A., Atinafu, D., Gao, H., Dong, W., and Wang, G. (2019). Shape-stabilized phase change materials based on porous supports for thermal energy storage applications. Chem. Eng. J. *356*, 641–661.

Huxtable, S.T., Cahill, D.G., Shenogin, S., Xue, L., Ozisik, R., Barone, P., Usrey, M., Strano, M.S., Siddons, G., Shim, M., and Keblinski, P. (2003). Interfacial heat flow in carbon nanotube suspensions. Nat. Mater. *2*, 731–734.

Ibrahim, N.I., Al-Sulaiman, F.A., Rahman, S., Yilbas, B.S., and Sahin, A.Z. (2017). Heat transfer enhancement of phase change materials for thermal energy storage applications: a critical review. Renew. Sustain. Energy Rev. *74*, 26–50.

Kim, K.S., Tarakeshwar, P., and Lee, J.Y. (2000). Molecular clusters of π-systems: theoretical studies of structures, spectra, and origin of interaction energies. Chem. Rev. *100*, 4145–4186.

Kim, T.Y., Park, C.-H., and Marzari, N. (2016). The electronic thermal conductivity of graphene. Nano Lett. *16*, 2439–2443.

Kong, W., Kum, H., Bae, S.-H., Shim, J., Kim, H., Kong, L., Meng, Y., Wang, K., Kim, C., and Kim, J. (2019). Path towards graphene commercialization from lab to market. Nat. Nanotechnol. *14*, 927–938.

Konuklu, Y., Ostry, M., Paksoy, H.O., and Charvat, P. (2015). Review on using microencapsulated phase change materials (PCM) in building applications. Energy Build. *106*, 134–155.

Latibari, S.T., and Sadrameli, S.M. (2018). Carbon based material included-shaped stabilized phase change materials for sunlight-driven energy conversion and storage: an extensive review. Sol. Energy *170*, 1130–1161.

Leong, K.Y., Rahman, M.R.A., and Gurunathan, B.A. (2019). Nano-enhanced phase change materials: a review of thermo-physical properties, applications and challenges. J. Energy Storage *21*, 18–31.

Li, C., Zhang, B., and Liu, Q. (2020b). N-eicosane/expanded graphite as composite phase change materials for electro-driven thermal energy storage. J. Energy Storage *29*, 101339.

Li, A., Dong, C., Dong, W., Yuan, F., Gao, H., Chen, X., Chen, X.-B., and Wang, G. (2020a). Network structural CNTs penetrate porous carbon support for phase-change materials with enhanced electro-thermal performance. Adv. Electron. Mater. *6*, 1901428.

Li, G., Hong, G., Dong, D., Song, W., and Zhang, X. (2018). Multiresponsive graphene-aerogel-directed phase-change smart fibers. Adv. Mater. *30*, 1801754.

Li, G., Zhang, X., Wang, J., and Fang, J. (2016). From anisotropic graphene aerogels to electron- and photo-driven phase change composites. J. Mater. Chem. A *4*, 17042–17049.

Li, M., and Mu, B. (2019). Effect of different dimensional carbon materials on the properties and application of phase change materials: a review. Appl. Energy *242*, 695–715.

Li, Y., Samad, Y.A., Polychronopoulou, K., Alhassan, S.M., and Liao, K. (2014). From biomass to high performance solar–thermal and electric–thermal energy conversion and storage materials. J. Mater. Chem. A *2*, 7759–7765.

Lin, Y., Jia, Y., Alva, G., and Fang, G. (2018). Review on thermal conductivity enhancement, thermal properties and applications of phase change materials in thermal energy storage. Renew. Sustain. Energy Rev. *82*, 2730–2742.

Liu, L., Alva, G., Huang, X., and Fang, G. (2016). Preparation, heat transfer and flow properties of microencapsulated phase change materials for thermal energy storage. Renew. Sustain. Energy Rev. *66*, 399–414.

Liu, P., Gao, H., Chen, X., Chen, D., Lv, J., Han, M., Cheng, P., and Wang, G. (2020a). In situ one-step construction of monolithic silica aerogel-based composite phase change materials for thermal protection. Compos. B Eng. *195*, 108072.

Liu, Z., Huang, Y., Huang, Y., Yang, Q., Li, X., Huang, Z., and Zhi, C. (2020b). Voltage issue of aqueous rechargeable metal-ion batteries. Chem. Soc. Rev. *49*, 180–232.

Liu, Z., Zou, R., Lin, Z., Gui, X., Chen, R., Lin, J., Shang, Y., and Cao, A. (2013). Tailoring carbon nanotube density for modulating electro-to-heat conversion in phase change composites. Nano Lett. *13*, 4028–4035.

Lu, X., Huang, H., Zhang, X., Lin, P., Huang, J., Sheng, X., Zhang, L., and Qu, J.-p. (2019). Novel light-driven and electro-driven polyethylene glycol/two-dimensional MXene form-stable phase change material with enhanced thermal conductivity and electrical conductivity for thermal energy storage. Compos. B Eng. *177*, 107372.

Lyu, J., Li, G., Liu, M., and Zhang, X. (2019a). Aerogel-directed energy-storage films with thermally stimulant multiresponsiveness. Langmuir *35*, 943–949.

Lyu, J., Liu, Z., Wu, X., Li, G., Fang, D., and Zhang, X. (2019b). Nanofibrous kevlar aerogel films and their phase-change composites for highly efficient infrared stealth. ACS Nano *13*, 2236–2245.

Maleki, M., Karimian, H., Shokouhimehr, M., Ahmadi, R., Valanezhad, A., and Beitollahi, A. (2019). Development of graphitic domains in carbon foams for high efficient electro/photo-to-thermal energy conversion phase change composites. Chem. Eng. J. *362*, 469–481.

Meschke, M., Guichard, W., and Pekola, J.P. (2006). Single-mode heat conduction by photons. Nature *444*, 187–190.

Min, P., Liu, J., Li, X., An, F., Liu, P., Shen, Y., Koratkar, N., and Yu, Z.Z. (2018). Thermally conductive phase change composites featuring anisotropic graphene aerogels for real-time and fast-charging solar-thermal energy conversion. Adv. Funct. Mater. *28*, 1805365.

Nazir, H., Batool, M., Osorio, F.J.B., Isaza-Ruiz, M., Xu, X., Vignarooban, K., Phelan, P., and Kannan, A.M. (2019). Recent developments in phase change materials for energy storage applications: a review. Int. J. Heat Mass Transfer *129*, 491–523.

Qiu, L., Ouyang, Y., Feng, Y., and Zhang, X. (2019). Review on micro/nano phase change materials for solar thermal applications. Renew. Energy *140*, 513–538.

Qureshi, Z.A., Ali, H.M., and Khushnood, S. (2018). Recent advances on thermal conductivity enhancement of phase change materials for energy storage system: a review. Int. J. Heat Mass Transfer *127*, 838–856.

Shaikh, S., Lafdi, K., and Hallinan, K. (2008). Carbon nanoadditives to enhance latent energy storage of phase change materials. J. Appl. Phys. *103*, 094302.

Shchukina, E., Graham, M., Zheng, Z., and Shchukin, D. (2018). Nanoencapsulation of phase change materials for advanced thermal energy storage systems. Chem. Soc. Rev. *47*, 4156–4175.

Sudeep, P.M., Narayanan, T.N., Ganesan, A., Shaijumon, M.M., Yang, H., Ozden, S., Patra, P.K., Pasquali, M., Vajtai, R., and Ganguli, S. (2013). Covalently interconnected three-dimensional graphene oxide solids. ACS Nano *7*, 7034–7040.

Sun, Q., Zhang, N., Zhang, H., Yu, X., Ding, Y., and Yuan, Y. (2020). Functional phase change composites with highly efficient electrical to thermal energy conversion. Renew. Energy *145*, 2629–2636.

Tabassum, H., Huang, X., Chen, R., and Zou, R. (2015). Tailoring thermal properties via synergistic effect in a multifunctional phase change composite based on methyl stearate. J. Materiomics *1*, 229–235.

Tarakeshwar, P., Choi, H.S., and Kim, K.S. (2001). Olefinic vs aromatic π−h interaction: a theoretical investigation of the nature of interaction of first-row hydrides with ethene and benzene. J. Am. Chem. Soc. *123*, 3323–3331.

Tian, X., Lu, X.F., Xia, B.Y., and Lou, X.W.D. (2020). Advanced electrocatalysts for the oxygen

reduction reaction in energy conversion technologies. Joule *4*, 45–68.

Tong, X., Li, N., Zeng, M., and Wang, Q. (2019). Organic phase change materials confined in carbon-based materials for thermal properties enhancement: recent advancement and challenges. Renew. Sustain. Energy Rev. *108*, 398–422.

Tsuzuki, S., Honda, K., Uchimaru, T., Mikami, M., and Tanabe, K. (2000). Origin of the attraction and directionality of the NH/π interaction: comparison with OH/π and CH/π interactions. J. Am. Chem. Soc. *122*, 11450–11458.

Umair, M.M., Zhang, Y., Iqbal, K., Zhang, S., and Tang, B. (2019a). Novel strategies and supporting materials applied to shape-stabilize organic phase change materials for thermal energy storage–A review. Appl. Energy *235*, 846–873.

Umair, M.M., Zhang, Y., Tehrim, A., Zhang, S., and Tang, B. (2020). Form-stable phase change composites supported by biomass-derived carbon scaffold with multiple energy conversion abilities. Ind. Eng. Chem. Res. *59*, 1393–1401.

Umair, M.M., Zhang, Y., Zhang, S., Jin, X., and Tang, B. (2019b). A novel flexible phase change composite with electro-driven shape memory, energy conversion/storage and motion sensing properties. J. Mater. Chem. A *7*, 26385–26392.

Wang, J., Jia, X., Atinafu, D.G., Wang, M., Wang, G., and Lu, Y. (2017a). Synthesis of "graphene-like" mesoporous carbons for shape-stabilized phase change materials with high loading capacity and improved latent heat. J. Mater. Chem. A *5*, 24321–24328.

Wang, X., Li, G., Hong, G., Guo, Q., and Zhang, X. (2017b). Graphene aerogel templated fabrication of phase change microspheres as thermal buffers in microelectronic devices. ACS Appl. Mater. Interfaces *9*, 41323–41331.

Wei, X., Xue, F., Qi, X.-D., Yang, J.-H., Zhou, Z.-W., Yuan, Y.-P., and Wang, Y. (2019). Photo- and electro-responsive phase change materials based on highly anisotropic microcrystalline cellulose/graphene nanoplatelet structure. Appl. Energy *236*, 70–80.

Wu, H., Deng, S., Shao, Y., Yang, J., Qi, X., and Wang, Y. (2019a). Multiresponsive shape-adaptable phase change materials with cellulose nanofiber/graphene nanoplatelet hybrid-coated melamine foam for light/electro-to-thermal energy storage and utilization. ACS Appl. Mater. Interfaces *11*, 46851–46863.

Wu, S., Yan, T., Kuai, Z., and Pan, W. (2019b). Thermal conductivity enhancement on phase change materials for thermal energy storage: a review. Energy Storage Mater. *25*, 251–295.

Wu, W., Huang, X., Li, K., Yao, R., Chen, R., and Zou, R. (2017). A functional form-stable phase change composite with high efficiency electro-to-thermal energy conversion. Appl. Energy *190*, 474–480.

Wu, Z.Y., Li, C., Liang, H.W., Chen, J.F., and Yu, S.H. (2013). Ultralight, flexible, and fire-resistant carbon nanofiber aerogels from bacterial cellulose. Angew. Chem. Int. Ed. *52*, 2925–2929.

Xu, Z., Zhang, Y., Li, P., and Gao, C. (2012). Strong, conductive, lightweight, neat graphene aerogel fibers with aligned pores. ACS Nano *6*, 7103–7113.

Xue, F., Jin, X.-Z., Wang, W.-Y., Qi, X.-D., Yang, J.-H., and Wang, Y. (2020). Melamine foam and cellulose nanofiber co-mediated assembly of graphene nanoplatelets to construct three-dimensional networks towards advanced phase change materials. Nanoscale *12*, 4005–4017.

Xue, F., Lu, Y., Qi, X.-D., Yang, J.-H., and Wang, Y. (2019). Melamine foam-templated graphene nanoplatelet framework toward phase change materials with multiple energy conversion abilities. Chem. Eng. J. *365*, 20–29.

Yang, G., Zhao, L., Shen, C., Mao, Z., Xu, H., Feng, X., Wang, B., and Sui, X. (2020). Boron nitride microsheets bridged with reduced graphene oxide as scaffolds for multifunctional shape stabilized phase change materials. Sol. Energy Mater. Sol. Cells *209*, 110441.

Yang, J., Qi, G.-Q., Bao, R.-Y., Yi, K., Li, M., Peng, L., Cai, Z., Yang, M.-B., Wei, D., and Yang, W. (2018). Hybridizing graphene aerogel into three-dimensional graphene foam for high-performance composite phase change materials. Energy Storage Mater. *13*, 88–95.

Yang, J., Qi, G.-Q., Liu, Y., Bao, R.-Y., Liu, Z.-Y., Yang, W., Xie, B.-H., and Yang, M.-B. (2016). Hybrid graphene aerogels/phase change material composites: thermal conductivity, shape-stabilization and light-to-thermal energy storage. Carbon *100*, 693–702.

Yu, J.-K., Mitrovic, S., Tham, D., Varghese, J., and Heath, J.R. (2010). Reduction of thermal conductivity in phononic nanomesh structures. Nat. Nanotechnol. *5*, 718–721.

Yuan, J., Chen, G., Weng, W., and Xu, Y. (2012). One-step functionalization of graphene with cyclopentadienyl-capped macromolecules via Diels–Alder "click" chemistry. J. Mater. Chem. *22*, 7929–7936.

Yuan, K., Shi, J., Aftab, W., Qin, M., Usman, A., Zhou, F., Lv, Y., Gao, S., and Zou, R. (2020). Engineering the thermal conductivity of functional phase-change materials for heat energy conversion, storage, and utilization. Adv. Funct. Mater. *30*, 1904228.

Zhang, H., Sun, Q., Yuan, Y., Zhang, Z., and Cao, X. (2018). A novel form-stable phase change composite with excellent thermal and electrical conductivities. Chem. Eng. J. *336*, 342–351.

Zhang, L., An, L., Wang, Y., Lee, A., Schuman, Y., Ural, A., Fleischer, A.S., and Feng, G. (2019a). Thermal enhancement and shape stabilization of a phase-change energy-storage material via copper nanowire aerogel. Chem. Eng. J. *373*, 857–869.

Zhang, L., Liu, X., Deb, A., and Feng, G. (2019b). Ice-templating synthesis of hierarchical and anisotropic silver-nanowire-fabric aerogel and its application for enhancing thermal energy storage composites. ACS Sustain. Chem. Eng. *7*, 19910–19917.

Zhang, Y., Umair, M.M., Zhang, S., and Tang, B. (2019c). Phase change materials for electron-triggered energy conversion and storage: a review. J. Mater. Chem. A *7*, 22218–22228.

Zhong, Y., Zhou, M., Huang, F., Lin, T., and Wan, D. (2013). Effect of graphene aerogel on thermal behavior of phase change materials for thermal management. Sol. Energy Mater. Sol. Cells *113*, 195–200.

Zhou, Y., Wang, X., Liu, X., Sheng, D., Ji, F., Dong, L., Xu, S., Wu, H., and Yang, Y. (2019). Polyurethane-based solid-solid phase change materials with halloysite nanotubes-hybrid graphene aerogels for efficient light-and electro-thermal conversion and storage. Carbon *142*, 558–566.

Zhou, Z., Zhang, Z., Zuo, J., Huang, K., and Zhang, L. (2015). Phase change materials for solar thermal energy storage in residential buildings in cold climate. Renew. Sustain. Energy Rev. *48*, 692–703.

Zhu, X., Han, L., Lu, Y., Wei, F., and Jia, X. (2019). Geometry-induced thermal storage enhancement of shape-stabilized phase change materials based on oriented carbon nanotubes. Appl. Energy *254*, 113688.